August 2019

Application of Geospatial Technologies for Land Use Analysis and Soil Science Education

Hamdi Zurqani
Clemson University, hzurqan@clemson.edu

APPLICATION OF GEOSPATIAL TECHNOLOGIES FOR LAND USE ANALYSIS AND SOIL SCIENCE EDUCATION

A Dissertation
Presented to
the Graduate School of
Clemson University

In Partial Fulfillment
of the Requirements for the Degree
Doctor of Philosophy
Forest Resources

---

by
Hamdi Abdalkhaliq Zurqani
December 2019

Accepted by:
Dr. Elena A. Mikhailova, Committee Chair
Dr. Christopher J. Post
Dr. Mark A. Schlautman
Dr. Julia L. Sharp

ABSTRACT

This research is composed of three parts: 1) Adaptation of Soil Judging to Libya, 2) Predicting the classes and distribution of salt-affected soils in Northwest Libya, and 3) Geospatial analysis of land use change in the Savannah River Basin using Google Earth. Soil judging (Evaluation) plays an important role in soil science education. Libya has six soil orders according to the U.S. Soil Taxonomy (Entisols, Aridisols, Alfisols, Inceptisols, Vertisols, and Mollisols) and the most common soil orders are Entisols and Aridisols. A Soil judging (Evaluation) scorecard was tested at two different universities in Libya: The University of Tripoli and University of Zawia. Eighty-two percent of Libyan users were not aware of Soil Judging prior to this study. After completing Soil Judging trials in various locations in Libya, ninety-five percent of those surveyed indicated that Soil Judging is useful to the natural science education. Libya is mostly a dry and arid country, where sodicity and salinity problems are often accelerated by the prevailing climatic condition and geographical setting of the area. A framework was identified for classifying and mapping salt-affected soils in northwest Libya using field measurements (ECe, soil pH, and SAR) and Geographic Information Systems (GIS). The majority of soils in this region of Libya are normal (slight degree of limitation). Twenty percent of the topsoil is saline-sodic (extreme degree of limitation). Land use change and the loss of wildlife habitats are serious issues facing the Southeastern United States. Across the Savannah River basin, the major change of land use was deforestation and reforestation during the entire study period with most of the changes located near lakes and water tributaries.

DEDICATION

To my parents, Abdalkhaliq and Mabrouka, and my lovely wife Nasrin, and my angels Yara, Sama, and Abdalrahman. To my brother, and sisters. Thank you for your love and emotional support throughout my graduate studies. Thank you all for giving me the strength to reach for the stars and chase my dreams.

ACKNOWLEDGMENTS

I would like to sincerely thank my committee members, Dr. Elena Mikhailova, Dr. Christopher Post, Dr. Mark Schlautman and Dr. Julia Sharp for their counsel, assistance and motivation throughout my Ph.D. studies. Also, I would like to extend my profound thanks to my country, Libya, the Libyan Government (Ministry of Higher Education and Scientific Research) on behalf of the University of Tripoli, and Clemson University for the financial support and resources I needed to finish my studies and accomplish my academic dream.

TABLE OF CONTENTS

Page

TITLE PAGE i

ABSTRACT ii

DEDICATION iii

ACKNOWLEDGMENTS iv

CHAPTER

I. INTRODUCTION 1

II. ADAPTATION OF SOIL JUDGING TO LIBYA 2

Abstract 2
Introduction 3
Materials and methods 5
Results and discussion 7
Conclusions 10
References 11
Appendix A 14

III. PREDICTING THE CLASSES AND DISTRIBUTION OF SALT-AFFECTED SOILS IN NORTHWEST LIBYA 28

Abstract 28
Introduction 30
Materials and methods 32
Results and discussion 37
Conclusions 40
References 42
Appendix A 49

IV. GEOSPATIAL ANALYSIS OF LAND USE CHANGE IN THE SAVANNAH RIVER BASIN USING GOOGLE EARTH ENGINE 59

Abstract 59
Introduction 61
Materials and methods 64

Results 72
Discussion 75
Conclusions 79
References 81
Appendix A 91
Appendix B 102

V. CONCLUSION 115

CHAPTER ONE

INTRODUCTION

The aims of this research are to introduce and discuss the application of soil sciences education and geospatial technologies to soils and land use. There are three main chapters of this research, starting with chapter, which describes the process of adapting Soil Judging (Evaluation) to Libya by enhancing the scorecard and adding more specific information relevant to Libya (e.g. soil salinity, calcium carbonate, etc.). The potential introduction of Soil Judging can be useful to students, governments, and the private sectors in Libya.

Chapter three discusses the development of the classification framework of the salt-affected soils in Libya based on electrical conductivity (ECe), soil pH, and the sodium adsorption ratio (SAR), and provides four degrees of limitations to salt-affected soils: slight (normal soils), moderate (saline soils), severe (sodic soils), and extreme (saline-sodic soils). This methodology can be applied to other arid regions around the world.

Chapter four discusses the advantage of utilizing the new geospatial technology of GEE and the historical record of Landsat satellite data to investigate the land use change within the Savannah River basin. The classes and the distribution of land cover in the area were determined to track and characterize changes in land use. This analysis helps to translate such information into assessments of current and historical land use change in the region and discusses its potential effects in the Savannah River basin.

CHAPTER TWO

ADAPTATION OF SOIL JUDGING (EVALUATION) TO LIBYA

Abstract

Adaptation of Soil Judging to Libya involves tailoring Soil Judging materials to local context of the country. The objectives of this study were to adapt Soil Judging to Libya and evaluate it in various locations in Libya. Various soil judging handbooks from the United States (US) were used to develop teaching materials for Libya (including tables of soil physical and chemical properties, topographic maps, and scorecards). The soil judging scorecard was enhanced by adding more specific information relevant to Libya (e.g. soil salinity, calcium carbonate etc.). Libyan users were asked to complete a survey consisting of questions related to the usefulness of Soil Judging in Libya. Eighty-two percent of those surveyed were not aware of Soil Judging prior to this study. After completing Soil Judging trials in various locations in Libya, 95% of those surveyed indicated that Soil Judging is useful to natural science education in Libya. Future improvements to Soil Judging should include better equipment and explanation.

Keywords: Africa; Agriculture; Environment; Education; Farming, Land use; Urbanization

Introduction

The first International Soil Judging Contest took place in June 2014 at the 20th World Congress of Soil Science in Korea with a limited number of countries participating in it (USA, Japan, China, Korea, South Africa, Australia, Taiwan, Mexico, Hungary, and the United Kingdom). Currently, Libya does not have Soil Judging can improve soil science knowledge exchange, and can potentially alleviate the problems of land use in Libya by teaching students and planners of important soil properties that limit land use such as: soil infiltration rate, hydraulic conductivity, available water, soil wetness class, and soil interpretations related to suitability for dwellings with basements, septic tank absorption field, and local roads and streets. Numerous studies documented various benefits of soil judging and field trips to enhance soil science learning in the US (Galbraith, 2012; Cavinder et al., 2011; Cooper and Dolan, 2003) and it would be beneficial to use this experience in other parts of the world.

Adaptation of educational materials to other countries is an important process, which can be divided into following steps: 1) identification of a reason for adaptation of environmental materials; 2) identification of people that need to be involved; 3) identification of important environmental issues; 4) identification of solutions to environmental problems; 5) identification, screening, and selecting environmental education materials; 6) copyright issues; 7) adapting and testing materials; 8) implementing an environmental education program; 9) evaluating a program and the effectiveness of adapted materials; 10) following principles of successful adaptation

(Peace Corps, 1999). Examples of adaptations of educational materials can range from lessons to programs (Peace Corps, 1999).

Soils in Libya are classified in accordance to the U.S. Soil Taxonomy (Zurqani *et al.*, 2019). Libya has six soil orders according to the U.S. Soil Taxonomy (Entisols, Aridisols, Alfisols, Inceptisols, Vertisols, and Mollisols) and the most common soil orders are Entisols and Aridisols (Zurqani *et al.*, 2012). Most Libyan soils have a sand or loamy sand texture with rapid soil infiltration (Nwer *et al.*, 2013). Maria *et al.* (2011) reported that rapid expansion of industry, urbanization and increasing population led to dramatic increases in the amount of municipal solid waste generated in Libya. Libyan soils are sands and loamy sands, they have very low available water and water stress is a common factor limiting crops yield especially in arid and semi-arid areas where the annual average precipitation does not exceed 300 mm (El-Assaad *et al*., 1992). Septic tanks are utilized in different regions of Libya, yet there is a lack of appropriate waste water collection and treatment facilities in the provincial zone, which could cause environmental issues.

Soil salinity problems in Libya result from low rainfall and high temperatures, extensive agricultural activities, overdraw of fresh groundwater, and seawater intrusion (Zurqani et al., 2012). Saline soils in Libya cover around 12 % of the north region, 16.5% of the west region and 23.4% of the middle region (Ben-Mahmoud, 1995). Sodicity also is common in semi-arid areas, particularly in sites where incoming water containing dissolved salt is lost by evaporation. The objectives of this study were to adapt Soil

Judging for Libya, conduct Soil Judging in various locations in Libya, and evaluate effectiveness of adapted materials using a survey.

Materials and Methods

Study area

Libya is situated in the northern portion of the African continent and covers 1,759,540 million km^2 (Zurqani *et al.*, 2019). Desert covers more than 95% of the country while cultivated areas cover slightly over 2% (Yigini *et al.*, 2013). Libya has an arid and semi-arid area climate influenced by the Mediterranean climate (Xeric), characterized by rainfall in the winter and almost no rainfall in the summer, which is the major heat and drought period of the year. The southern part of Libya, however, is under the (Torric) moisture regime (Ben-Mahmoud, 1995).

The average monthly temperatures range from 13.2 C° to 27.9 C° with an annual level of 20.7 C°, and the soil temperature regime in the study area is thermic (Ben-Mahmoud, 1995). The average annual rainfall varies from region to region according to the geographic position and the topography. Rainfall occurs during the winter months (October to March) (Zurqani *et al.*, 2012). Land degradation and desertification are the main soil threats facing agricultural development.

Soil Judging Equipment and Materials

Most Soil Judging equipment can be acquired in Libya or ordered from providers. Analyses of soil physical and chemical properties can be obtained from any one of the many soil nutrient analysis laboratories in Libya: Libyan Universities Institutes, and Libyan Agriculture Research Centers.

Courses Background

A soil judging course can be integrated into various soil science programs currently being taught in Libya, for example: University of Tripoli, Omar Al-Mukhtar University, Sebha University, Al Zawia University , Sirte University , University of Elmergib, University of Al Jabal Al Gharbi, Higher Institute of agricultural techniques (Al_Gheiran, Tripoli). All of these institutions can use soil judging to improve the soil courses such as Fundamentals of Soil Science course or in a more specific course such as Soil Survey Genesis and Classification course. Soil judging education can directly benefit the agriculture, housing and city planning, transportation, and health services. Computer laboratories and internet services in most of Libyan universities can be used in creating Modular Object-Oriented Dynamic Learning Environment (Moodle). This environment could be used for e-learning learning (e.g. storing course materials, and evaluating students learning through electronic tests and quizzes).

Results and Discussion

Libya-specific Modifications to Soil Judging Scorecard

The main soil orders in Libya are Entisols, Aridisols, Mollisols, Alfisols, Vertisols, and Inceptisols (Ben-Mahmoud, 1995; Soil Survey Staff, 2003). Generally, aside from the Jabal Akhdar and a portion of the Tripoli Mountains (Jabal Nafusah), the most common soil orders are Entisols and Aridisols (Zurqani *et al.,* 2019). Dry climatic conditions in Libya result in high accumulation of calcium carbonate, and the presence of gypsum in some areas (Zurqani *et al.,* 2019). The precipitation and accumulation of calcium carbonate may result in the development of calcic/petrocalcic horizons that vary in the extent of their development depending on the circumstances and composition (Ben-Mahmoud, 1995). According to Ben-Mahmoud (1995) these soils generally cover large areas in the northern region of the country. In order to adapt soil judging scorecard to Libya, the following additions/modification were made to the already existing soil judging scorecard: adding, a column for test of carbonates, plant sensitivity to salt affected soils (Table 1), and wind erosion potential classes (Table 2).

A newly developed soil judging scorecard (Fig. 1A and 1B) is adapted for Libyan soils classified using USDA/SCS Soil Taxonomy. In order to demonstrate how to use soil judging scorecard, soil pit No. 3 (Zurqani, 2010) was used to fill out the "practice" soil scorecard (Fig. 1A and 1B). In addition to the soil judging scorecard, other supplemental materials were used: 1) Soil physical and chemical properties (Fig. 2), 2) optional topographic map of the area (Fig. 3), 3) textural triangle (not shown, but it is the same

used in Libya and USA), 4) abbreviations of distinctness of soil boundary, texture, modifiers of rock fragment quantity and size, structure grade, structure shape, consistence, redoximorphic features (Table 3), 5) tables of surface and soil erosion potential classes, and 6) tables of soil use interpretations for dwellings with basement, septic absorption fields, and local roads and streets. Soil pit No. 3, which was one of soil profiles conducted by Zurqani (2010) in the northwest of Libya near the coastal strip. The soil pit has been classified as Natric Petrocalcids in the USDA/SCS Soil Taxonomy (1999. In part B, the infiltration rate was determined to be medium based on soil texture (LS/S) and soil organic carbon content (0.19%) in the Ap horizon (Karathanasis *et al*., 2013). Hydraulic conductivity was determined to be low based on subsurface horizon characteristics (Karathanasis *et al*., 2013). Available water was calculated based on depth of 70 cm x 0.05 = 3.5 cm (multiplier for LS and LS/S in all of the horizons) (Karathanasis *et al*., 2013). The soil wetness class is > 150 cm (not wet at depths of less than 151 cm) because of lack of redoximorphic features through the soil pit (Karathanasis *et al*., 2013). Soil interpretation for dwellings with basements was identified as "2 = moderate" based on using the following criteria: flooding or ponding (none), slope (< 6 %), depth to seasonally high water table (> 100 cm), and depth to duripan layer (kqm) (50 - 100 cm), and depth to hard rock, R (cm) > 150 cm. Soil interpretation for septic tank absorption fields was identified as "3 = severe", based on using the following criteria: flooding or ponding (none), slope (< 6 %), depth to seasonally high water table (> 150 cm), the limiting hydraulic conductivity "low", and depth to duripan layer (kqm) 50 - 100 cm, and depth to hard rock, R (cm) > 150 cm. Soil interpretation for local roads and

streets was identified as “2 = moderate” based on using the following criteria: flooding or ponding (none), slope (< 6 %), depth to seasonally high water table (> 100 cm), and depth to duripan layer (kqm) 50 - 100 cm, and depth to hard rock, R (cm) > 150 cm. Soil interpretation for plant sensitivity to salt affected soils was “4 = extreme” based on the surface horizon, and using the following criteria: pH = 7.1, SAR (%) = 22.04, and the ECe (dS/m) = 4.

In Part C, surface runoff class was “slow” based on > 1 – 2 % slope and “medium” infiltration determined in the Part B of the scorecard. In Part C, erosion potential was “very low” based “slow” surface runoff and LS/S surface horizon texture determined in the Part A of the scorecard.

Application of Soil Judging in Libya

The soil judging scorecard was tested and evaluated at two different universities in Libya using Soil Judging survey form (Table 4): University of Tripoli, and University of Zawia. Soil Judging was conducted by professors in the departments of soil science in Libyan universities by various participants: 54% were students, 23% were researchers, 10% were educators, and 10% were workers. Fifty percent of participants had a high school degree, 35% had a bachelor’s degree, 11% had a master’s degree, and four percent had a doctorate. Initially, participants were asked about their knowledge of soil science: 73% responded that they had a soil science course before and 40% indicated that they had conducted field work related to soil science. Eighty-two percent of participants stated that they had no prior knowledge of Soil Judging, and 95% stated that Soil Judging is useful

to natural science education in Libya (Table 5). Adapted materials (e.g. scorecard) and explanatory materials were evaluated between "good" and "excellent" (Table 6). The evaluation of the soil judging equipment was between "poor" and "good" (Table 6).

Specific feedback from the participants is valuable to provide more specific guidelines on positive and negative aspects of the project (Table 7). Responses included the desire for additional seminars to increase the awareness and potential impact of Soil Judging in Libya as well as including additional field locations. Access to equipment including soil pH and EC tests was listed as a need.

Conclusions

Adaptation of Soil Judging to Libya involves tailoring Soil Judging materials to local context of the country. This article describes adaptation and evaluation of Soil Judging materials in Libya. A survey provided after the Soil Judging trials in Libya showed that 82% of respondents never knew about Soil Judging and 95% of those surveyed indicated that Soil Judging is useful to natural science education in Libya. Libya has the necessary resources to successfully introduce soil judging competitions to schools (middle and high schools, colleges, and universities), and various government agencies. Soil nutrient analysis information can be acquired from any of the soil nutrient analysis laboratories in Libya.

References

Blanco-Canqui, H., & Lal, R. (2008). Principles of soil conservation and management. Springer Science & Business Media.

Cavinder, C.A., B. Byrd, J. Franke, and G. Holub. 2011. "Texas A&M University student life skill development and professional achievement from participation on a collegiate judging team." NACTA Journal. 55:60–62.

Cooper, T.H., and M. Dolan. 2003. "TEAM and individual scores at the 2002 national soil judging contest." Journal of Natural Resources and Life Sciences Education. 32:20–22.

Galbraith, J.M. 2012. "Using student competition field trips to increase teaching and learning effectiveness." Journal of Natural Resources & Life Sciences Education. 41:54–58.

Food and Agriculture Organization (FAO). 2005. "AQUASTAT country profile: Libyan Arab Jamahiriya. Land and Water Division." Food and Agriculture Organization of the United Nations. Rome. ftp://ftp.fao.org/agl/aglw/docs/wr29_eng.pdf (last accessed on 02/26/16).

Karathanasis, A.D., Galbraith, J.M., Shaw, J.N. and Thompson, J.A. 2013. "Handbook for Collegiate Soils Contest." Southeast Region Web Site: http://gis.clemson.edu/elena/documents/SE_Handbook_2013.pdf (last accessed on 02/26/16).

Ludwig, B., Boiffin, J., Chad, J., & Auzet, A. V. (1995). Hydrological structure and erosion damage caused by concentrated flow in cultivated catchments. Catena, 25(1), 227-252.

Ben-Mahmoud, K. 1995. “Libyan Soils.” First Edition. Tripoli: National Research Scientific Organization.

Maria, G. A. Omran, and A. Salahalddin. 2011. “Municipal solid waste management in Bani Walid City, Libya: practices and challenges.” Journal of Environmental Management and Tourism. No. 10. 228-237

Nwer, B., H, Zurqani and K, Judour. 2013. “Soil Productivity Rating Index Model Using Geographic Information System in Libya.” Annual International Conference 7th Edition of Geotunis, Tunis.

Peace Corps, 1999. “Adapting Environmental Education Materials.” Washington, DC. Information Collection and Exchange Div." http://files.peacecorps.gov/multimedia/pdf/library/M0059_adaptenviron.pdf (last accessed on 01/23/17).

Selkhozpromexport. 1980. “Soil Studies in the Eastern zone of the Socialist People′s Libyan Arab Jamahiriya.” Secretariat for Agricultural Reclamation and Land Development, Tripoli.

Siewert, Christian, Pavel Barsukov, Scott Demyan, Andrey Babenko, Nikolay Lashchinsky, and Elena Smolentseva. 2014. “Teaching soil science and ecology in West Siberia: 17 years of field courses.” Environmental Education Research 20, no. 6 :858-876.

Yigini, Y., Panagos, P. and Montanarella, L., 2013. “Soil resources of mediterranean and Caucasus countries.” Office for Official Publications of the Euroean Communities, Luxembourg. http://eusoils.jrc.ec.europa.eu/ESDB_Archive/eusoils_docs/other/EUR25988EN.pdf (last accessed on 02/28/16).

Soil Survey Staff. 2003. “Natural Resources Conservation Service, United States Department of Agriculture.” Keys to Soil Taxonomy. 9th ed. USDA. Washington, DC.

Zurqani, H.A. 2010. “Determination of Spreading and Interference Magnitude of Marshes Soils in North-western Areas of Libya Using Remote Sensing (RS) and Geographic Information Systems (GIS).” Master thesis. University of Tripoli.

Zurqani, H., B. Nwer, and E, Rhoma. 2012. “Assessment of Spatial and Temporal Variations of Soil Salinity using Remote Sensing and Geographic Information System in Libya.” Annual International Conference and Earth Science (GEOS) 3-4 December 2012 Singapore. http://dl4.globalstf.org/?wpsc-product=assessment-of-spatial-and-temporal-variations-of-soil-salinity-using-remote-sensing-and-geographic-information-system-in-libya (last accessed on 02/28/16).

Zurqani, H.A., Mikhailova, E.A., Post, C.J., Schlautman, M.A. and Elhawej, A.R., 2019. A Review of Libyan Soil Databases for Use within an Ecosystem Services Framework. Land, 8(5), p.82

APPENDIX A

Table 1. Plant Sensitivity to salt affected soils (Adapted from Brady and Weil, 2007).

	Degree of limitation			
Factors affecting use	**Slight (1) (Normal Soils)**	**Moderate (2) (Saline Soils)**	**Severe (3) (Sodic Soils)**	**Extreme (4) (Saline-Sodic Soils)**
1. pH	< 8.5	< 8.5	> 8.5	< 8.5
2. SAR (%)	0 - 13	0 - 13	13 – 50 (or more)	13 – 50 (or more)
3. ECe (dS/m)	0 – 4	4 - 14	0 - 4	4 - 14

Table 2. Wind erosion potential classes. Adopted from (Blanco-Canqui et al. 2008)[1], (Ludwig et al. 1995)[2].

Factors influence wind Erosion relative to the surface horizon texture (Barriers[1], surface roughness[2]**)**	**Wind Erosion Potential Classes**				
	Surface horizon texture class[3]				
	L, (SiL > 20 % clay), CL, Si, SiCL,	L, (SiL < 20 % clay), SCL, SC	C, SiC, CL, (SiCL > 35 % clay)	L, SL, SiC, CL,	S, LS
- Vegetative barriers with feedlot windbreak - Very rough Soil surface	Very low	Very low	Very low	Low	Low
- Vegetative barriers (perennial plants or annual plants combination) - Rough Soil surface	Low	Low	Low	Medium	Medium
- Strip Cropping - Medium Soil surface	Medium	Medium	Medium	High	High
- Lack of crop residue - Smooth Soil surface	High	High	High	Very high	Very high
- Bare soil - Very smooth Soil surface	Very high	Very high	Very high	Very high	Very high

Notes: this table didn't take in the consideration of the slope and the water quantity in the surface horizon.

Table 3. Abbreviations (Adapted from Handbook for Collegiate Soils Contest, 2011).

Distinctness of Boundary			
Abrupt = A	Gradual = G		
Clear = C	Diffuse = D		
Texture			
Sand = S	Silt = Si	Clay = C	Loam = L
Sandy Loam = SL	Silt Loam = SiL	Clay Loam = CL	Sandy Clay = SC
Sandy Clay Loam = SCL	Silty Clay Loam = SiCL		Loamy Sand = LS
Sandy Clay = SC	Silty Clay = SiC		
Modifiers of Rock Fragment Quantity and Size			
Gravelly = GR	Cobbly = CB	Stony = ST	
Very Gravelly = VGR	Very Cobbly = VCB	Very Stony = VST	
Extr. Gravelly = XGR	Extr. Cobbly = XCB	Extr. Stony = XST	
Structure Grade			
Structureless = SLS	Weak = WK	Moderate = MO	Strong = ST
Structure Shape			
Granular = GR	Prismatic = PR	Angular Blocky = ABK	
Platy = PL	Single Grain = SG	Subangular Blocky = SBK	
Massive = MA			
Consistence			

Loose = L	Friable = FR	Very Friable = VFR
Firm = Fi	Very Firm = VFi	Extremely Frim = EFi

Redoximorphic Features

Enter “Yes” (Y) if present, and “No” if none are present.

presence or absence of carbonates (e.g. CaCO3)

Effervescence class	Criteria
Non effervescent (N)	No bubbles detected
Very slightly effervescent (VSli)	Few bubbles seen
Slightly effervescent (Sli)	Bubbles readily seen
Strongly effervescent (St)	Bubbles from low foam
Violently effervescent (Vio)	Thick foam from quickly

Table 4. Soil Judging survey form.

Soil Judging Survey

Thank you for participating in this Survey of "Potential Adaptation of Soil Judging in Libya." Your responses will be very useful in further improvement and development of this project.

Please, fill in the bubble with your answers ●or circle the appropriate answer.

Part A. General Information.

I am a: ○ student; ○ farmer; ○ worker; ○ engineer; ○ educator; ○ researcher; ○ other

My highest education is: ○ school; ○ university; ○ M.S; ○ Ph.D.; ○ other: _____

My academic major or specialty is: _____

1. Have you ever had a soil science course? (Yes / No)
2. Have you ever had field work related to soil science? (Yes / No)

Part B. Questions about Soil Judging power point presentation.

3. Did you find the Soil Judging power point presentation informative?
   1 = not at all 3 = somewhat 5 = very informative
4. How did you find quality of explanation?
   1 = poor 3 = good 5 = excellent
5. Did you know about Soil Judging before this power point presentation? (Yes / No)
6. Is Soil Judging useful to natural science education in Libya? (Yes / No)?
7. Please, provide specific comments about further improvements to this power point presentation:

Part C. Questions about field demonstration:

8. Did you find the field demonstration for Soil Judging informative?
   1 = not at all 3 = somewhat 5 = very informative
9. How did you find quality of field demonstration and explanation?
   1 = poor 3 = good 5 = excellent
10. Please, provide specific comments about further improvements to this field

demonstration and explanation:

Part D. Questions about field work.

11. Did you find the Soil Judging field work informative?

    1 = not at all 3 = somewhat 5 = very informative

12. How did you find quality of Soil Judging equipment?

    1 = poor 3 = good 5 = excellent

13. How did you find quality of the Soil Judging scorecard?

    1 = poor 3 = good 5 = excellent

14. Please, provide specific comments about further improvements to field work related to Soil Judging:

Table 5. Responses from Libyan users to questions about the Soil Judging project (total number of participants = 53).

Survey questions	Yes (%)	No (%)	N/A†
1. Have you ever had a soil science course? (Yes / No)	73	27	-
2. Have you ever had field work related to soil science? (Yes / No)	40	60	1
3. Did you know about Soil Judging before this power point presentation? (Yes / No)	18	82	3
4. Is Soil Judging useful to natural science education in Libya? (Yes / No)	95	5	1

† N/A = not answered.

Table 6. Responses about the quality of the Soil judging (total number of participants = 53).

Survey question	Mean ± SD†	N/A†
15. Did you find the Soil Judging power point presentation informative? (1 = not at all, 3 = somewhat, 5= very informative)	4.5 ± 0.8	-
16. How did you find quality of explanation? (1 = poor, 3 = good, 5 = excellent)	3.7 ± 1.0	-
17. Did you find the field demonstration for Soil Judging informative? (1 = not at all, 3 = somewhat, 5 = very informative)	4.6 ± 0.9	1
18. How did you find quality of field demonstration and explanation? (1 = poor, 3 = good, 5 = excellent)	3.8 ± 1.0	1
19. Did you find the Soil Judging field work informative? (1 = not at all, 3 = somewhat, 5 = very informative)	4.5 ± 0.9	-
20. How did you find quality of Soil Judging equipment? (1 = poor, 3 = good, 5 = excellent)	2.0 ± 1.0	1
21. How did you find quality of the Soil Judging scorecard? (1 = poor, 3 = good, 5 = excellent)	4.4 ± 1.0	2

† SD = standard deviation; N/A = not answered.

Table 7. Specific recommendations to improve Soil Judging in Libya.

Do you have any suggestion to improve the adaptation of Soil Judging power point presentation (or suggestion for other "field demonstration and explanation" and "field work related to Soil Judging")
1. You should organize conferences and seminars about soil judging that will raise awareness about how it is importance and how it is work for soil evaluation as big part of applied science. 2. I hope if you organize field trips and visits to different fields to practices on with different types of soil and places. 3. I wish next would visit we have the necessary support for equipment and transportation. 4. You should seek to teach soil judging approach as field practices will help students recognize the importance of soil and study its various properties evaluated. 5. It was very informative that will help me on both sides an academic and field work in my M.S. research. 6. We need to know more details about Soil Judging. 7. We need more field work. 8. Provide all the equipment that we needed in soil judging test. 9. Provide the hand measurement for the soil pH test and Soil EC test will help us a lot.
This is my first time I visit the field to study soil properties and I like it a lot.

No. of Horizons 3
Depth to be described 70 cm
Nail in 3rd horizon @ 60 cm

Contestant _____

A. Morphology

Horizon						Texture			Color			Structure		Consist.	Redox. Features			CaCO3	Score
Pre.	Master	Sub	No.	Lower depth	Bound. distnct.	Rock fragmnt modif.	USDA class	Clay content	Hue	Val.	Chr.	Grade	Shape	Moist	Redox conc. y/n	Redox depltn. y/n	Red. matrix y/n	HCl 1N (N, Vsli, Sli, St, Vio)	
1	3	2	1	3	1	1	3	1	1	1	1	2	2	1	1	1	1	3	30
-	A	p	-	20	C	-	LS	2.2	7.5YR	5	4	SLS	MA	L	N	N	N	Vio	
-	C	-	1	50	C	-	LS/S	6	7.5YR	5	4	SLS	MA	L	N	N	N	Vio	
-	C	-	2	70+	-	-	-	-	-	-	-	-	-	-	-	-	-	-	

B. Soil Profile and Interpretations

Infiltration Rate (5)
____ Rapid
_X_ Medium
____ Slow

Available Water (5)
_X_ Very Low ≤ 7.5 cm
____ Low > 7.5 and ≤ 15.0 cm
____ Moderate > 15.0 and ≤ 22.5 cm
____ High > 22.5 cm

Soil Interpretations (2 each)
_2_ Dwellings with Basements
_3_ Septic Tank Absorption Field
_2_ Local Roads and Streets
_4_ Plant Sensitivity to salt affected soils
(1 = slight, 2 = moderate, 3 = severe, 4 = Extreme)

Part A _____
Part B _____
Part C _____
Part D _____
Total _____

Hydraulic Conductivity (5)
____ High
____ Moderate
_X_ Low

Soil Wetness Class (5)
_X_ > 150 cm
____ 101-150 cm
____ 51-100 cm
____ 25-50 cm
____ < 25 cm

Figure 1 (A). Example of the front side of completed scorecard for the soil pit No. 3 in Zuwarah, Libya (scorecard adapted from Karathanasis et al., 2011).

C. Site Characteristics

Position of Site (5)
_____ Depression
_____ Drainage Way
_____ Flood Plain
_____ Footslope
_____ Stream Terrace
__X__ Upland

Parent Material (5)
_____ Alluvium
_____ Colluvium
_____ Residuum
__X__ Loess

Soil Slope (5)
__X__ Nearly Level (0 to 2%)
_____ Gently Sloping (>2 to 6%)
_____ Sloping (>6 to 12%)
_____ Moderately Sloping (>12 to 20%)
_____ Strongly Sloping (>20 to 30%)
_____ Steep (>30%)

Surface Water Runoff (5)
_____ Ponded
_____ Very Slow
__X__ Slow
_____ Medium
_____ Rapid
_____ Very Rapid

Wind Erosion Potential (5)
_____ Very Low
_____ Low
_____ Medium
_____ High
__X__ Very High

Water Erosion Potential (5)
__X__ Very Low
_____ Low
_____ Medium
_____ High
_____ Very High

Part C Score _____

D. Soil Classification

Epipedons (5)
_____ Mollic
__X__ Ochric
_____ Umbric
_____ Anthropic

Subsurface Horizons
and Characteristics (5 each)
_____ Albic
_____ Argillic
_____ Cambic
_____ Calcic
__X__ Petrocalcic
_____ Gypsic
_____ Petrogypsic
_____ Natric
_____ Salic
_____ Duripan
_____ Fragipan
_____ Lithologic Discontinuit
_____ Lithic Contact
_____ Paralithic Contact
_____ None

Order (5)
_____ Alfisols
_____ Entisols
_____ Inceptisols
_____ Mollisols
_____ Vertisols
__X__ Aridisols

Part D Score _____

Figure 1 (B). Example of the back side of completed scorecard for the soil pit No. 3 in Zuwarah, Libya (scorecards adapted from Karathanasis et al., 2011).

PIT No. 3
No. of horizons 3
Depth to be described 70 cm
Nail in 3rd horizon @ 60 cm

HORIZON	OC (%)	BS (meq/L)	pH	$CaCO_3$ (%)	SAR (%)	ECe (dS/m)
1	0.19	29.21	7.1	38.51	22.04	4.00
2	0.01	3.37	7.5	36.75	15.85	0.25
3	-	-	-	-	-	-

Flooding: None Ponding: None

Figure. 2. Soil physical and chemical properties for the soil profile No. 3 in Zuwarah, Libya.

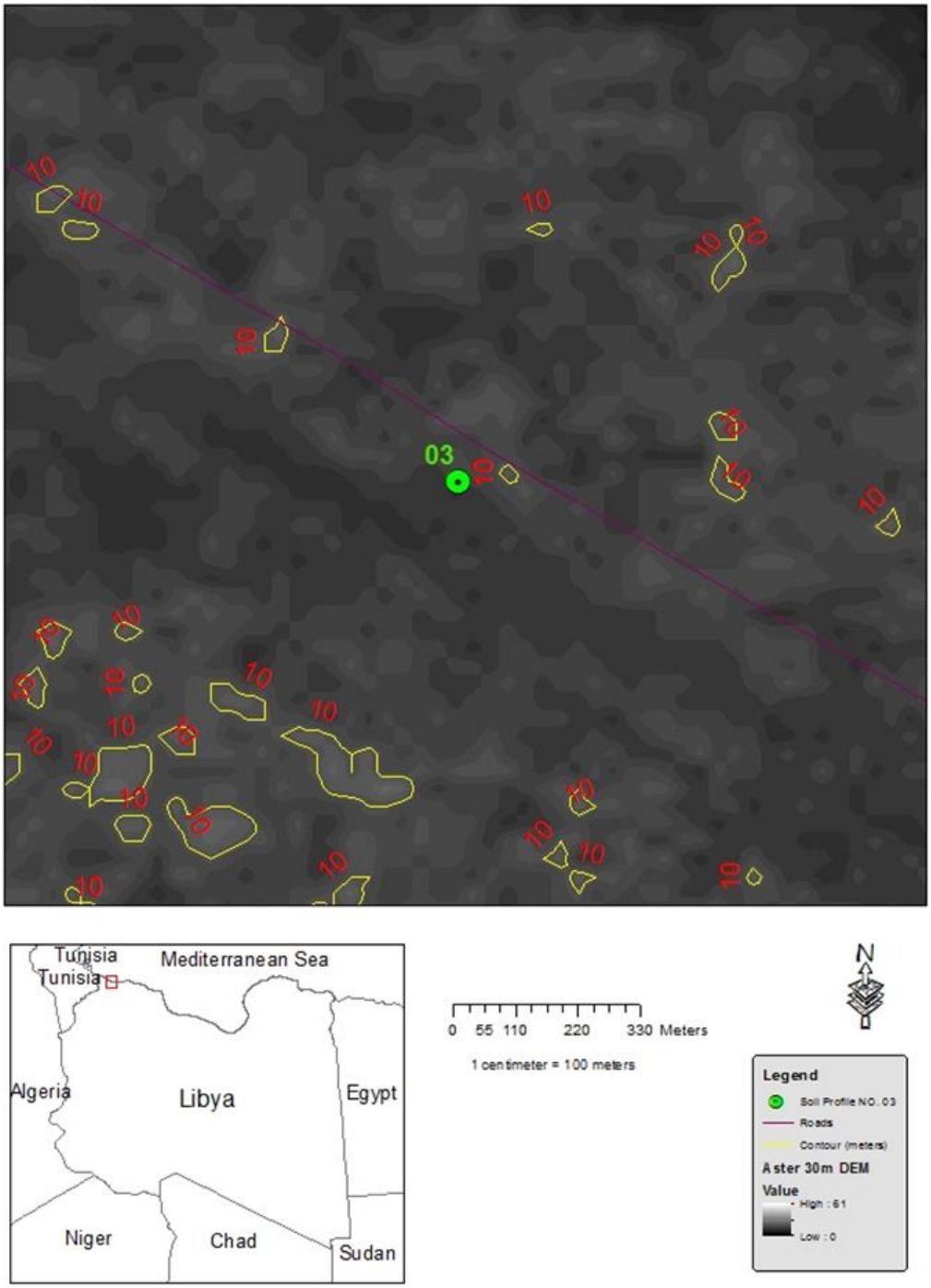

Figure. 3. Topographic map for the soil profile No. 3 in Zuwarah, Libya.

CHAPTER THREE

PREDICTING THE CLASSES AND DISTRIBUTION OF SALT-AFFECTED SOILS IN NORTHWEST LIBYA

This chapter is based on:

Zurqani, H.A, Mikhailova, E.A., Post, C.J., Schlautman, M.A., and J.L Sharp. 2018. Predicting the classes and distribution of salt-affected soils in Northwest Libya. Commun. Soil Sci. Plant Anal. 49(6):689-700.

Abstract

Sodicity and salinity can adversely affect soil structure and are common constraints to plant growth in arid regions. Current remote sensing techniques cannot distinguish between the various classes of salt-affected soils. Field and laboratory measurements of salt-affected soils are time-consuming and expensive. Mapping of the salt-affected soils can be used in soil conservation planning to identify regions with different degrees of limitations. There is a need to use existing field and laboratory measurements to create maps of classes of salt-affected soils. The objectives of this study are to classify salt-affected soils, use existing field data to interpolate and validate geospatial predictions of the classes of salt-affected soils using Geographic Information Systems (GIS), and create maps showing the different classes and distribution of salt-affected soils. The classification framework for salt-affected soils is based on electrical conductivity (ECe), soil pH and the sodium adsorption ratio (SAR) and provides four degrees of limitations to salt-affected soils: slight (normal soils), moderate (saline soils), severe (sodic soils), and extreme (saline-sodic soils). Spatial interpolation of the field data from northwestern Libya was verified by cross-validation, and maps of the salt-affected soils in the region

were created. The majority of soils in this region of Libya are normal (slight degree of limitation). Twenty percent of the topsoil is saline-sodic (extreme degree of limitation). Land use recommendations and rehabilitation strategies can be developed from such maps of salt-affected soil classes. The methodology followed in this study can be applied to other arid regions around the world, particularly in developing countries where budgetary constraints limit detailed field and laboratory measurements of sodicity and salinity.

Keywords: Electrical conductivity (ECe) of water-saturated soil paste; geographic information system (GIS); inverse distance weighting (IDW); mean error (ME); sodium adsorption ratio (SAR); normalized (N); root mean square error (RMSE)

Introduction

Natural and/or human-induced salinization and sodification processes that adversely affect soil structure and limit or restrict plant growth are common in arid regions (Qadir, Ghafoor, and Murtaza 2001; Shrivastava and Kumar 2015; Tejedor, Jiménez, and Díaz 2003). The ions primarily responsible for salinization ("saline" soil) are the cations sodium (Na^{+}), potassium (K^{+}), calcium (Ca^{2+}) and magnesium (Mg^{2+}) and the anions chloride (Cl^{-}), sulfate (SO_4^{2-}), bicarbonate (HCO^{3-}), and carbonate (CO_3^{2-}). If Na+ predominates in the soil, the soil becomes "sodic" (Abrol, Yadav, and Massoud 1988; Hamza 2008; Provin and Pitt 2001). Sodic soils are characterized by a poor soil structure, a low infiltration rate, poor aeration and are difficult to cultivate (Qadir and Schubert 2002). Saline and sodic soils can significantly reduce the value and productivity of affected land (Metternicht and Zinck 2003). For example, the economic damage caused by secondary salinization in the Colorado River Basin was estimated at $750M (million US dollars) per year (Iqbal 2011; Iqbal and Mastorakis 2015). Different approaches are used to solve different salinity- and sodicity associated problems (Shrivastava and Kumar 2015), including leaching (Callaghan, Cey, and Bentley 2014), application of organic waste products (Ghosh et al. 2010), and use of volcanic mulch (Tejedor, Jiménez, and Díaz 2003). The USDA Soil Salinity Laboratory (Richards 1954) has developed salinity classification system based on the electrical conductivity of the saturation extract (ECe, in dS/m at 25 C°), the exchangeable sodium

percent (ESP) or sodium adsorption ratio (SAR) to classify among saline, saline-alkaline, and alkaline soils. Plyusnin (1964) developed a classification system based on salt types (e.g., chloride, sulfate, etc.). Monitoring soil salinity and sodicity requires knowledge of their magnitude and associated spatial and temporal variability (Douaik, Van Meirvenne, and Tóth 2007). Because field and laboratory measurements of electrical conductivity and other pertinent soil properties can be time-consuming and expensive, significant research has been conducted using statistical methods (Douaik, Van Meirvenne, and Tóth 2007), remote sensing (Goldshleger et al. 2010; Seifert, Ortiz-Monasterio, and Lobell 2011), and mapping techniques (Zare et al. 2015) to aid in the management of salt affected soils and to enhance the speed, accuracy, and cost-effectiveness of rehabilitation strategies (Metternicht and Zinck 2003). Remote sensing has been used to detect soil salinity (Eldeiry and Garcia 2008), but challenges remain to identify or distinguish the different classes of salt-affected soils. Metternicht (2001) assessed temporal and spatial changes of salinity using fuzzy logic, remote sensing, and GIS in the Punata-Cliza Valley, Bolivia. Metternicht (2003) used a classification based on anion ratios (Plyusnin 1964) and integrated it into the class boundary modeling for mapping salt-affected soils using Landsat TM data. The adverse effects of salinity and sodicity on plant growth and development are a major problem limiting agricultural production in Libya (Läuchli and Grattan 1969). More than three decades ago, it was estimated that the area covered by saline soils was about 2000 km2 in the northwestern part of Libya and over 3000 km2 in the northeastern part of the country (Selkhozpromexport 1980). Saline soils in Libya cover around 12% of the north region, 16.5% of the west region and 23.4% of the middle

region (BenMahmoud 1995). Since then, Zurqani, Nwer, and Rhoma (2012) assessed the spatial and temporal variations of soil salinity in Libya using remote sensing and GIS but without linking those variations to the classes of salt-affected soils. Based on soil pH, ECe and SAR, the current study proposes to create a classification framework that will provide four degrees of limitations for salt-affected soils: slight (normal soils), moderate (saline soils), severe (sodic soils), and extreme (saline-sodic soils) (Brady and Weil 2008). Integration of field and laboratory data with geospatial analysis provides a unique opportunity to create a user accessible map of the classes of salt-affected soils in Libya. Several studies to determine soil salinity in he north-western part of Libya have been performed (LIB/00/004 2007, 2009; NCB, 2004; Nwer, Zurqani, and Rhoma 2014), but none connected their results to the classes of salt-affected soils. The objectives of this study were to: (1) use a framework to classify salt-affected soils using Geographic Information Systems (GIS), (2) validate geospatial predictions of the classes of salt affected soils using existing field data, and (3) create maps of salt-affected soils for the study area.

Materials and Methods

Study area

The study area is located in northwest Libya in the Zuwarah region (12° 16′ 01″ to 11° 48′ 35″ E and 32° 30′ 33″ to 32° 59′ 44″ N) (Figure 1). The study area totals about 134,000 hectares (NCB, 2004) and is part of the Al-Jafarah plain, considered to be the most important agricultural region in the country. The study area has a Mediterranean

climate, with average monthly temperatures ranging from 13.2°C to 27.9°C and an average annual temperature of 20.7°C (Zurqani, Nwer, and Rhoma 2012). Most of the yearly rainfall occurs during the winter months (October to March) with great temporal and spatial variability.

The study area is a part of the largest contiguous salt-affected area in the north-west of Libya. Most of the soils in the region are undeveloped or partly developed with Aridisols and Entisols being the main soil orders (Table 1) in the study area (Ben Mahmoud, 1995; Zurqani, Nwer, and Rhoma 2012).

Soil profile descriptions

Data for fourteen soil profiles were reported by NCB (2004) (Table 1). Each map unit/great group contained two or more soil profiles. Soil samples were collected to the depth 150 cm unless hard– cemented layer "duripans" were present or the sampler reached groundwater. Electrical conductivity of 1:1 saturated extracts (ECe) was measured with an electrical conductivity detector and results were expressed in dS/m at 25 C° (NCB, 2004). Soil pH was measured in 1:1 aqueous soil extracts with a pH meter and electrode (NCB, 2004). Exchangeable cations were extracted by an ammonium acetate solution, measured with a flame atomic absorption spectrophotometer, and reported in milliequivalent/100 g soil (NCB, 2004). Soil sodicity was reported as the exchangeable sodium percent (ESP). Because the sodium adsorption ratio (SAR) is a widely utilized index used to distinguish soil sodicity, we calculated SAR from ESP with the following set of equations (Havlin et al. 2005):

$$ESP = \frac{(\text{Exchangeable } Na^{+})}{\text{CEC}} \times 100 \quad (1)$$

$$ESP = (100 \times \text{ESR}) / (1 + \text{ESR}) \quad (2)$$

$$SAR = \text{ESR} / 0.015 \quad (3)$$

where *ESP* is the exchangeable sodium percent, CEC is the cation exchange capacity, ESR is the exchangeable sodium ratio, and *SAR* is the sodium adsorption ratio.

Geospatial analysis

The spatial distribution of salt-affected soils was analyzed using ArcGIS 10.3 spatial analyst tool (Table 2; Figure 2) (ESRI, 2014). The classes of salt-affected soils were classified based on ECe, pH, and SAR values (Table 3). In this study, spatial interpolation was performed using inverse distance weighting (IDW) to estimate data values for the locations where measured values for the topsoil and subsoil properties (e.g., EC_e, pH, SAR) were not available. Inverse distance weighted interpolation, which explicitly assumes that soils that are close to one another are more alike in their properties than are soils that are farther apart, is one of the most commonly-used spatial interpolation methods for visualizing the continuity and variability of observed data across a surface (Robinson, and Metternicht, 2006). A common formulation for IDW interpolation is (Burrough and McDonnell., 1998):

$$\hat{y}(x_0) = \frac{\sum_{i=1}^{n} y(x_i) d_{0,i}^{-r}}{\sum_{i=1}^{n} d_{0,i}^{-r}} \quad (4)$$

where x_0 is the estimation point/location and x_i are the locations of data points within a chosen neighborhood where measured soil properties (e.g., $y(x_i)$) are available. The estimated soil property value ($\hat{y}(x_0)$) is determined from the neighborhood values ($y(x_i)$), which are weighted by the inverse of the distance between the estimation point and neighborhood points ($d_{0,i}$) raised to a selected power (r). The IDW formula has the effect of giving data points close to the interpolation point relatively large weights while those far away exert less influence. The higher the power used, the more influence that points closer to x_0 are given. Default settings in ArcGIS were used to determine IDW interpolation maps using the fourteen soil sample locations across the entire study area. Among the default settings were inverse distance squared weighting (i.e., power value of 2) from the twelve nearest sampling points.

Statistical and validation analyses

Summary statistics were calculated using geostatistical tools in ArcGIS 10.3. The maps of the soil profiles data (pH, ECe, and SAR) (Figure 3) that were used to generate subsequent maps of the classes of salt-affected soils were validated using a leave-one-out cross-validation (LOOCV) procedure to assess the interpolation accuracy of the final maps. In the cross-validation procedure, one soil sample was removed and a calibration map was developed from the remaining soil samples (i.e., the 13 remaining soil samples) (Fig. 2a). The LOOCV procedure was used for each soil variable (pH, ECe, and SAR). Assessment of the LOOCV procedure utilized the mean error (ME), root mean square error (RMSE) and normalized RMSE (NRMSE) (Li and Heap, 2011):

$$ME = \frac{1}{n}\sum_{i=1}^{n}(p_i - o_i) \quad (5)$$

$$RMSE = \left[\frac{1}{n}\sum_{i=1}^{n}(p_i - o_i)^2\right]^{1/2} \quad (6)$$

$$NRMSE = \frac{RMSE}{o_{i,max} - o_{i,min}} \quad (7)$$

where n is the number of locations for the observations/samples; o_i signifies the observed/measured values, p_i signifies the predicted/estimated values, and $o_{i,max}$ and $o_{i,min}$ are the maximum and minimum observed values, respectively. In general, values of ME, RMSE and NRMSE that are closer to zero indicate a higher validity for the IDW interpolation maps. In addition, positive or negative values for ME indicate whether bias exists in the predicted values.

Results and Discussion

Framework and classes of salt affected soils

The proposed framework classifies salt affected soils (based on ECe, soil pH, and SAR) and was used to map salt affected soils using a case study in Libya. In this study, a framework provides four classes of salt-affected soils: slight (normal soils), moderate (saline soils), severe (sodic soils), and extreme (saline-sodic soils) (Table 3). Three interpolation maps of ECe; soil pH; and SAR Fig 3a,b,c were developed to classify salt affected soils using the proposed framework.

Traditionally, geospatial technologies (including remote sensing) have been widely used to detect salt affected soils based on just one individual soil property (e.g., ECe, soil color etc.) without taking into consideration the combination of multiple soil properties (Metternicht and Zinck., 2003; Farifteh et al., 2006; Farifteh et al., 2008; Mulder et al., 2011; Muller and Niekerk, 2016). Electrical conductivity (ECe) has traditionally been used to detect and classify salt affected soils using remote sensing techniques because it can be detected from soil surface reflectance (Metternicht and Zinck, 2003; Eldeiry and Garcia, 2008; Goldshleger et al., 2010; Allbed and Kumar, 2013). Soil pH was used to predict soil alkalinity and salinity in the Wuyu'er-Shuangyang River Basin, Northeast China (Bai et al., 2016). Nield et al. (2007) digitally mapped gypsic and natric soils using Landsat ETM data based on SAR. Heilig et al. (2011) evaluated potential of using electromagnetic induction to characterize and map sodium-affected soils in the Northern Great Plains. Heilig et al. (2011) used stochastic models to predict SAR and ECe and classified the soils into four different classes, but without including soil pH as a factor for the classification.

Sarani et al. (2015) predicted ESP and SAR from EC and pH data using artificial neural network and regression models. Continuous monitoring of salt affected areas requires rapid updating (Farifteh et al. 2006), and that can be effectively done using remote sensing techniques (Allbed et al., 2013).

The current study proposes a framework that combines multiple soil properties (ECe, soil pH, and SAR) to classify the salt-affected soils in the topsoil and subsoil, which is more difficult to predict using only remotely sensed data. The main limitation of the proposed framework is that it relies on laboratory measurements, which are expensive and time-consuming especially for large areas.

Evaluation of predicted data

A cross-validation procedure was conducted to check the geospatial accuracy between the measured data and the IDW estimates. The accuracy was assessed using the root mean square error (RMSE), and mean error (ME) (Table 4), where values close to zero indicate higher validity. Soil pH interpolation maps for both top and subsoil had the highest validity by given an accurate RMSE (0.46 and 0.20) with ME (0.05 and 0.04), respectively. The current study found that the ECe were high in the topsoil and subsoil with RMSE (8.78, and 9.90 dS m^{-1}), and ME (1.08, and 0.83 dS m^{-1}), respectively. The SAR had the highest RMSE (13.11) and biased ME (1.99) in the topsoil and more accurate RMSE (4.98) with ME unbiased (0.27) in the subsoil. The current study used validation techniques commonly reported in salinity research. For example, a study conducted in northeastern China (Bai et al., 2016) assessed the map accuracies generated from the Operational Land Imager (OLI)

using 14 soil samples. Bai et al. (2016) found the soil pH estimation reaching the RMSE of (1.01). Heilig et al. (2011) used stochastic models to predict the SAR and ECe in Northern Great Plains, USA from the EC data of 18 soil samples in two different sites for the 0–30, 30–60, 60–90 cm depth intervals for 2 fields: field 1 (ECe RMSE: 0.92, 3.70, and 6.43 dS $m^{-}1$; SAR (3.52, 9.71, and 7.67), and field 2 (ECe RMSE: 3.84, 2.39, and 5.77 dS $m^{-}1$; SAR (2.51, 4.23, and 5.86) (Heilig et al., 2011).

The current study identified that evaluation of the interpolation map predictions from soil profiles is complicated by the fact that ECe and SAR have a wide range of values. To account for these wide ranges, the RMSE values were normalized by the range to obtain NRMSE (equation 7). The lower values of NRMSE (Table 4) in both top and subsoil with range 0.20 to 0.31 indicates less residual variance for ECe, pH, and SAR. Many researchers have used a cross-validation procedure to make comparisons between the estimated and measured soil data collected in the laboratory to validate the accuracy of an interpolation estimates (Voltz and Webster, 1990; Robinson and Metternicht, 2006; Hengl et al., 2015). The validation of the maps indicated that salt-affected soils classes can be generated reliably from the new framework. Measurement of soil data and interpolation using IDW will enhance the digital mapping of salt-affected soils.

Salt-affected soils in Libya

The classes of salt-affected soils as shown in (Fig. 4a, b) and (Table 5). The topsoil (Fig. 4a) with slight degree (normal soils) covered approximately 77% of the study area, where the extreme degree (saline-sodic) soils covered about 18%, and the moderate degree

(saline soils) covered only 3%. There is a small area of slight degree (normal soils) shown in the map that have a pH more than 8.5 that do not meet the other characters to be considered as severe degree (sodic soils). Also, there is an area that has ECe less than 4 and SAR more than 13, but the soil pH is less than 8.5 which does not meet all the factors to consider the soil as severe degree (sodic soils). These unidentified areas covered about 2% of the area.

In the subsoil (Figure 4b) the slight degree (normal soils) covered approximately 69% of the area, while the moderate degree (saline soils) covered about 29%. The extreme degree (saline-sodic soils) covered 1%. These maps (Figure 4a-d) provide an insight on the distribution of the classes of salt-affected soils at different depths for monitoring and management of salt-affected soils (Metternicht and Zinck, 2003).

Conclusions

This study identified a framework for classifying and mapping salt-affected soils using field measurements (ECe, soil pH, and SAR) and Geographic Information Systems (GIS). The framework suggests four degrees of limitations to salt-affected soils: slight (normal soils), moderate (saline soils), severe (sodic soils), and extreme (saline-sodic soils). Spatial interpolation of the field data was verified by cross validation, and maps of the salt-affected soils in the region were created. The reason for the high values of RMSE, and ME of ECe and SAR particularly in the topsoil was likely because of the small number of the soil profiles that were used and the wide-ranging values of the ECe and SAR in the

soil data. The majority of the soils in this region of Libya are normal (slight degree of limitation). Twenty percent of the topsoil is saline-sodic (extreme degree of limitation). Since field data collection is expensive and time-consuming, future research needs should focus on using remote sensing techniques for soil pH and SAR predictions.

References

Abrol, I. P., J. S. P. Yadav, and F. I. Massoud. 1988. Salt-Affected Soils and Their Management. Food and Agriculture Organization of the United Nations, Rome.

Allbed, A., and L. Kumar. 2013. Soil salinity mapping and monitoring in arid and semi-arid regions using remote sensing technology: A review. Advances in Remote Sensing 02(04):373–385. doi:10.4236/ars.2013.24040

Bai, L., C. Wang, S. Zang, Y. Zhang, Q. Hao, and Y. Wu. 2016. Remote sensing of soil alkalinity and salinity in the Wuyu'er-Shuangyang River Basin, Northeast China. Remote Sensing 8(2):163. doi:10.3390/rs8020163

Ben-Mahmoud, K B. 1995. Libyan Soils. First Edition ed. Tripoli: National Research Scientific Organization.

Brady, N. C., and R. R. Weil. 2008. The Nature and Properties of Soils. 13th edition. Prentice Hall, Upper Saddle River, New Jersey 07458.

Buck, B. J., J. King, and V. Etyemezian. 2011. Effects of salt mineralogy on dust emissions, Salton Sea, California. Soil Science Society of America Journal 75(5): 1971-1985. doi:10.2136/sssaj2011.0049

Burrough, P. A., and R. A. McDonnell. 1998. Creating continuous surfaces from point data. Principles of Geographic Information Systems. Oxford University Press, Oxford, UK.

Callaghan, M. V., E. E. Cey, and L. R. Bentley. 2014. Hydraulic conductivity dynamics during salt leaching of a sodic, structured subsoil. Soil Science Society of America Journal 78:1563-1574. doi:10.2136/sssaj2014.03.0106

Douaik, A., M. Van Meirvenne, and T. Tóth. 2007. Statistical methods for evaluating soil salinity spatial and temporal variability. Soil Science Society of America Journal 71: 1629-1635. doi:10.2136/sssaj2006.0083

Eldeiry, A. A., and L. A. Garcia. 2008. Detecting soil salinity in alfalfa fields using spatial modeling and remote sensing. Soil Science Society of America Journal 72:201-211. doi:10.2136/sssaj2007.0013

ESRI World Imagery Map Service/ Digital Globe. 2010.

ESRI. 2014. ArcGIS Desktop: Release 10.3. Redlands, CA: Environmental Systems Research Institute.

Farifteh, J., A. Farshad, and R. George. 2006. Assessing salt-affected soils using remote sensing, solute modelling, and geophysics. Geoderma 130(3-4):191–206 doi:10.1016/j.geoderma.2005.02.003

Farifteh, J., F. V. D. Meer, M. V. D. Meijde, and C. Atzberger. 2008. Spectral characteristics of salt-affected soils: A laboratory experiment. Geoderma 145(3-4): 196–206. doi:10.1016/j.geoderma.2008.03.011

Ghosh, S., P. Lockwood, N. Hulugalle, H. Daniel, P. Kristiansen, and K. Dodd. 2010. Changes in properties of sodic Australian Vertisols with application of organic waste products. Soil Science Society of America Journal 74:153-160. doi:10.2136/sssaj2008.0282

Goldshleger, N., E. Ben-Dor, R. Lugassi, and G. Eshel. 2010. Soil degradation monitoring by remote sensing: Examples with three degradation processes. Soil Science Society of America Journal 74:1433-1445. doi:10.2136/sssaj2009.0351

Hamza, M. A. 2008. Understanding Soil Analysis Data. Resource Management technical report 327. Dept. Of agriculture and food government of western Australia. ISSN 1039-7205

Havlin, J. L., J. D. Beaton, S. L. Tisdale, and W. L. Nelson. 2005. Soil Fertility and Fertilizers: An Introduction to Nutrient Management. 7th ed. Pearson Prentice Hall, Upper Saddle River, NJ.

Heilig, J., J. Kempenich, J. Doolittle, E. C. Brevik, and M. Ulmer. 2011. Evaluation of electromagnetic induction to characterize and map sodium-affected soils in the Northern Great Plains. Soil Horizons 52(3):77. doi:10.2136/sh2011.3.0077

Hengl, T., G. B. M. Heuvelink, B. Kempen, J. G. B. Leenaars, M. G. Walsh, K. D. Shepherd, A. Sila, R. A. Macmillan, J. M. D. Jesus, L. Tamene, and J. E. Tondoh. 2015. Mapping soil properties of Africa at 250 m resolution: Random forests significantly improve current predictions. PLOS ONE 10(6). doi:10.1371/journal.pone.0125814

Iqbal, F. 2011. Detection of salt affected soil in rice-wheat area using satellite image. African Journal of Agricultural Research 6:4973-82.

Iqbal, S., and N. Mastorakis. 2015. Soil salinity detection using RS data. In: Advances in Environmental Science and Energy Planning. 277-281. ISBN 978-1-61804-280-4.

Läuchli, A., and S. Grattan. 1969. Plant Growth and Development under Salinity Stress. Advances in Molecular Breeding toward Drought and Salt Tolerant Crops: 1–32. doi:10.1007/978-1-4020-5578-2_1 http://www.redsalinidad.com.ar/assets/files/revisiones/lauchli%20grattan.pdf

Li, J., and A. D. Heap. 2011. A review of comparative studies of spatial interpolation methods in environmental sciences: Performance and impact factors. Ecological Informatics 6(3-4):228–241. doi:10.1016/j.ecoinf.2010.12.003

LIB/00/004. 2007. Mapping of natural resource for agriculture use and mapping project document (GAA, FAO, and UNDP). http://www.glcn.org/activities/libya_en.jsp

LIB/00/004. 2009. Atlas of natural resources for agricultural use in Libya. http://www.fao.org/documents/card/en/c/afa20dd0-7f4a-4e11-beb9-d9b3b79e0e65/

Metternicht, G. 1998. Fuzzy classification of JERS-1 SAR data: an evaluation of its performance for soil salinity mapping. Ecological Modelling 111:61-74.

Metternicht, G. 2001. Assessing temporal and spatial changes of salinity using fuzzy logic, remote sensing and GIS. Foundations of an expert system. Ecological Modelling 144(2-3):163-179.

Metternicht, G. 2003. Categorical fuzziness: a comparison between crisp and fuzzy class boundary modelling for mapping salt-affected soils using Landsat TM data and a classification based on anion ratios. Ecological Modelling 168: 371-389.

Metternicht, G., and J. Zinck. 2003. Remote sensing of soil salinity: potentials and constraints. Remote Sensing of Environment 85(1):1–20. doi:10.1016/s00344257(02)00188-8

Mulder, V., S. D. Bruin, M. Schaepman, and T. Mayr. 2011. The use of remote sensing in soil and terrain mapping — A review. Geoderma 162(1-2):1–19. doi:10.1016/j.geoderma.2010.12.018

Muller, S. J., and A. V. Niekerk. 2016. An evaluation of supervised classifiers for indirectly detecting salt-affected areas at irrigation scheme level. International Journal of Applied Earth Observation and Geoinformation 49:138–150. doi:10.1016/j.jag.2016.02.005

National Consulting Bureau (NCB). 2004. Technical studies on soil survey and classification in coastal areas of the north-western of Libya on behalf of General Water Authority of Libya (Field data of the report Stage IV: Final Report). http://www.ncblibya.com/index.html

Nield, S. J., J. L. Boettinger, and R. D. Ramsey. 2007. Digitally mapping gypsic and natric soil areas using Landsat ETM data. Soil Science Society of America Journal 71(1):245-252.

Nwer, B., H. Zurqani, and E. Rhoma. 2014. The use of remote sensing and geographic information system for soil salinity monitoring in Libya. GSTF Journal of Geological Sciences 1(1) doi:10.5176/2335-6774_1.1.5

Plyusnin, I. 1964. Reclamative Soil Science. Foreign Languages Publishing House, Moscow

Provin, T., and J. L. Pitt. 2001. Managing Soil Salinity. Texas AgriLife Extension Service publication E-60. Texas A&M Univ. Publication. College Station, TX. [Online] http://soiltesting.tamu.edu/publications/E-60.pdf.

Richards, L. 1954. United States salinity laboratory staff, diagnosis and improvement of saline and alkali soils. In: Richards, L. (Ed.), Agriculture Handbook No. 60, US Department of Agriculture, USA.

Qadir, M., A. Ghafoor, and G. Murtaza. 2001. Use of saline–sodic waters through phytoremediation of calcareous saline–sodic soils. Agricultural Water Management 50(3): 197–210. doi:10.1016/s0378-3774(01)00101-9

Qadir, M., and S. Schubert. 2002. Degradation processes and nutrient constraints in sodic soils. Land Degradation and Development 13(4):275–294. doi:10.1002/ldr.504

Robinson, T., and G. Metternicht. 2006. Testing the performance of spatial interpolation techniques for mapping soil properties. Computers and Electronics in Agriculture 50(2): 97–108. doi:10.1016/j.compag.2005.07.003

Sarani, F., A. G. Ahangar, and A. Shabani. 2015. Predicting ESP and SAR by artificial neural network and regression models using soil pH and EC data (Miankangi region, Sistan and Baluchestan provice, Iran). Archives of Agronomy and Soil Science 62(1): 150414060638008. DOI: 10.1080/03650340.2015.1040398

Seifert, C., J. I. Ortiz-Monasterio, and D. B. Lobell. 2011. Satellite-Based Detection of Salinity and Sodicity Impacts on Wheat Production in the Mexicali Valley. Soil Science Society of America Journal 75(2): 699. doi:10.2136/sssaj2010.0233

Selkhozpromexport. 1980. Soil Studies in the Eastern zone of the Socialist People′s Libyan Arab Jamahiriya. Secretariat for Agricultural Reclamation and Land Development, Tripoli.

Shrivastava, P., and R. Kumar. 2015. Soil salinity: A serious environmental issue and plant growth promoting bacteria as one of the tools for its alleviation. Saudi Journal of Biological Sciences 22(2):123–131. doi:10.1016/j.sjbs.2014.12.001

Tejedor, M., C. C. Jiménez, and F. Díaz. 2003. Use of volcanic mulch to rehabilitate saline-sodic soils. Soil Science Society of America Journal 67(6):1856. doi:10.2136/sssaj2003.1856

Voltz, M., and R. Webster. 1990. A comparison of kriging, cubic splines and classification for predicting soil properties from sample information. European Journal of Soil Science 41(3):473–490. doi:10.1111/j.1365-2389.1990.tb00080.x

Zare, E., J. Huang, F. M. Santos, and J. Triantafilis. 2015. Mapping salinity in three dimensions using a DUALEM-421 and electromagnetic inversion software. Soil Science Society of America Journal 79(6):1729. doi:10.2136/sssaj2015.06.0238

Zurqani, H., B. Nwer, and E. Rhoma. 2012. Assessment of Spatial and Temporal Variations of Soil Salinity using Remote Sensing and Geographic Information System in Libya. Conference Proceedings on 1st Annual International Conference on Geological & Earth Sciences. doi:10.5176/2251-3361_geos12.64 http://dl4.globalstf.org/?wpsc-product=assessment-of-spatial-and-temporal-variations-of-soil-salinity-using-remote-sensing-and-geographic-information-system-in-libya

APPENDIX A

Table 1 Selected chemical and physical properties of the measured soil profiles (NCB, 2004).

No. (ID)	Topsoil				Subsoil				Soil profile classification†
	pH	ECe	SAR	Texture class	pH	ECe	SAR	Texture class	
	(-)	dS/m	(-)		(-)	dS/m	(-)		
1 (004)	8.02	6.65	15.43	Sand	7.81	35.88	10.88	Loamy Sand	Typic Aquisalids
2 (050)	7.66	0.49	5.89	Loamy Sand	8.02	8.33	2.50	Loamy Sand	Haplosalidic Torriorthents
3 (090)	7.99	4.37	50.09	Sand	7.97	22.61	7.27	Loamy Sand	Typic Haplosalids
4 (153)	7.21	0.32	6.26	Sand	7.40	0.37	7.61	Loamy Sand	Typic Haplocalcids
5 (221)	7.62	0.30	4.49	Loamy Sand	7.71	0.27	18.75	Loamy Sand	Typic Torripsamments
6 (167)	8.4	30.3	29.53	Sand	8.0	19.21	3.48	Sand	Typic Haplosalids
7 (349)	7.58	0.35	4.45	Sand	7.90	0.23	4.64	Sand	Typic Torripsamments
8 (378)	8.94	0.36	3.21	Sand	8.13	0.31	18.72	Sand	Typic Torripsamments
9 (271)	7.92	0.91	4.01	Sand	7.91	0.74	3.88	Sand	Typic Torripsamments
10 (560)	7.52	1.14	3.87	Sand	7.67	1.24	2.23	Sand	Typic Torripsamments
11 (958)	8.22	0.22	4.77	Sand	7.74	1.77	4.84	Loamy Sand	Typic Petrogypsids
12 (042)	7.96	0.23	3.93	Sand	8.02	0.29	3.54	Sand	Typic Torripsamments
13 (116)	8.0	0.26	4.09	Sand	7.61	0.33	6.45	Sand	Typic Haplosalids
14 (218)	7.9	0.26	3.90	Loamy Sand	7.72	0.27	4.41	Sand	Typic Haplosalids

† Soil profile classification at the great group level (NCB, 2004).

Table 2 Data sources and descriptions.

Data Layer	Source	Coordinate System	Date
Digital data set	LIB/00/004 Mapping of Natural Resources for Agriculture Use and Planning in Libya.	GCS_WGS_1984	2007
Aerial imagery	Satellite imagery for the world and high-resolution	ESRI World Imagery Map Service/ Digital Globe	2010

Table 3 Classes of salt affected soils (adapted from Brady and Weil, 2008).

Factors affecting use	Degree of limitation			
	Slight (1) (Normal soils)	**Moderate (2) (Saline soils)**	**Severe (3) (Sodic soils)**	**Extreme (4) (Saline-Sodic soils)**
ECe (dS/m)	< 4	≥ 4	< 4	≥ 4
pH	< 8.5	< 8.5	≥ 8.5	< 8.5
SAR	< 13	< 13	≥ 13	≥ 13

Table 4 Summary statistics of measured soil properties and model cross validation results for ECe, pH, and SAR.

		Measured					Cross-validation			
Depth	**Soil Property**	**Min**	**Max**	**Range**	**Mean**	**Median**	**SD†**	**RMSE‡**	**ME§**	**NRMSE¶**
Topsoil (n=14)	ECe (dS/m)	0.22	30.30	30	3.30	0.36	8.00	8.78	1.08	0.29
	pH	7.21	8.94	2	7.93	7.96	0.42	0.46	0.05	0.23
	SAR	3.21	50.09	47	10.28	4.47	13.48	13.11	1.99	0.27
Subsoil (n=14)	ECe (dS/m)	0.23	35.88	36	6.56	0.56	11.23	9.90	0.83	0.28
	pH	7.40	8.13	1	7.83	7.86	0.19	0.20	0.04	0.20
	SAR	2.23	18.72	16	6.02	4.53	4.33	4.98	0.27	0.31

† Standard deviation.
‡ RMSE=Root Mean Square Error.
§ Mean Error.
¶ Normalized Root Mean Square Error=NRMSE.

Table 5 Distribution of soil types (NCB, 2004) and classes of salt affected soils in the study area.

Soil type	Area	Topsoil				Subsoil			
		Degree of limitation				Degree of limitation			
		Slight (Normal soils)	Moderate (Saline soils)	Extreme (Saline-Sodic soils)	Not identified†	Slight (Normal soils)	Moderate (Saline soils)	Extreme (Saline-Sodic soils)	Not identified‡
	ha (%)	%							
Typic Torripsamments†	103243 (77)	89.0	1.6	6.5	2.9	78.7	19.9	0.4	1.0
Typic Haplocalcids	3600 (2.7)	7.8	0.0	92.2	0.0	5.3	94.7	0.0	0.0
Typic Aquisalids	9420 (7.0)	35.0	3.8	59.7	1.5	22.9	77.1	0.0	0.0
Typic Haplosalids	9858 (7.4)	68.8	0.0	31.2	0.0	87.0	13.0	0.0	0.0
Haplosalidic Torriorthents	2640 (2.0)	29.5	0.0	69.8	0.7	8.7	91.3	0.00	0.00
Typic Petrogypsids	5239 (3.9)	59.3	0.0	40.7	0.0	62.8	37.2	0.00	0.00
		ha							
Total area	134000 (100)	103976	3756	23439	2874	93053	39547	430	1017

†Typic Torripsamments are including the urban areas.

‡Not identified (these areas that not matched with any classes of salt affected soils).

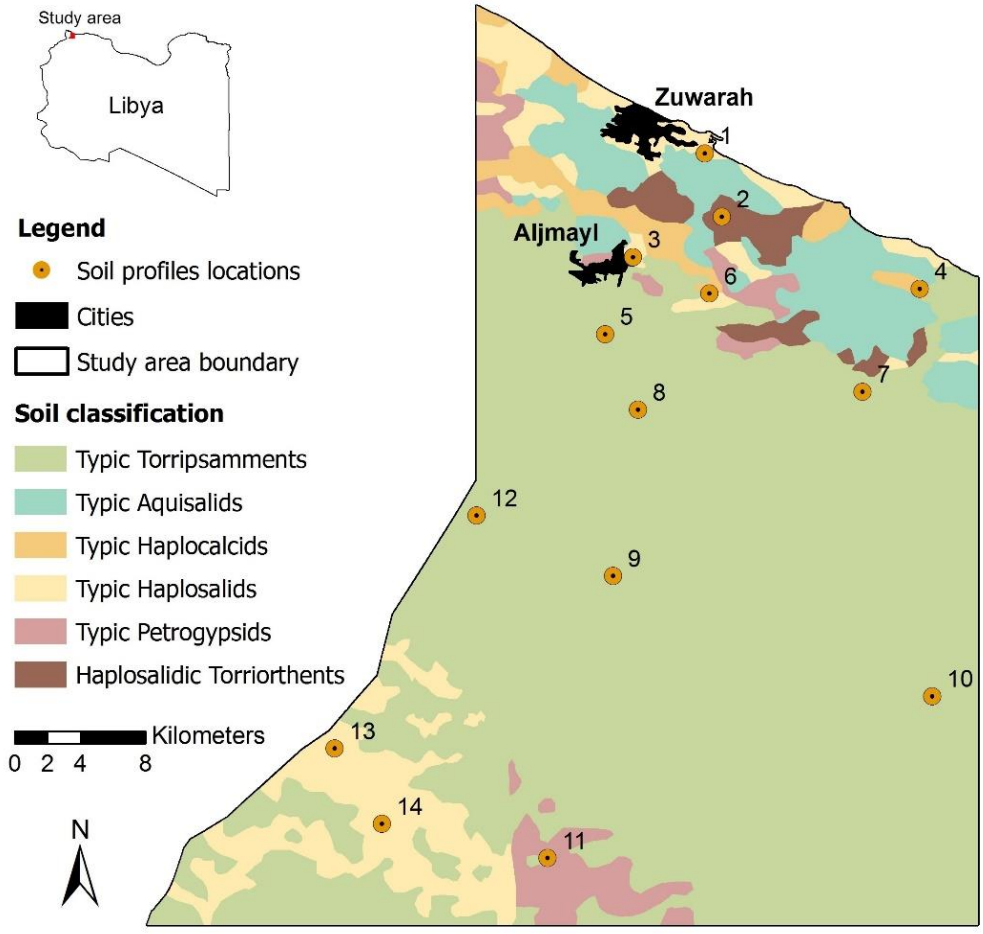

Figure 1. Map of the study area and soil profile locations in Northwest Libya (NCB, 2004).

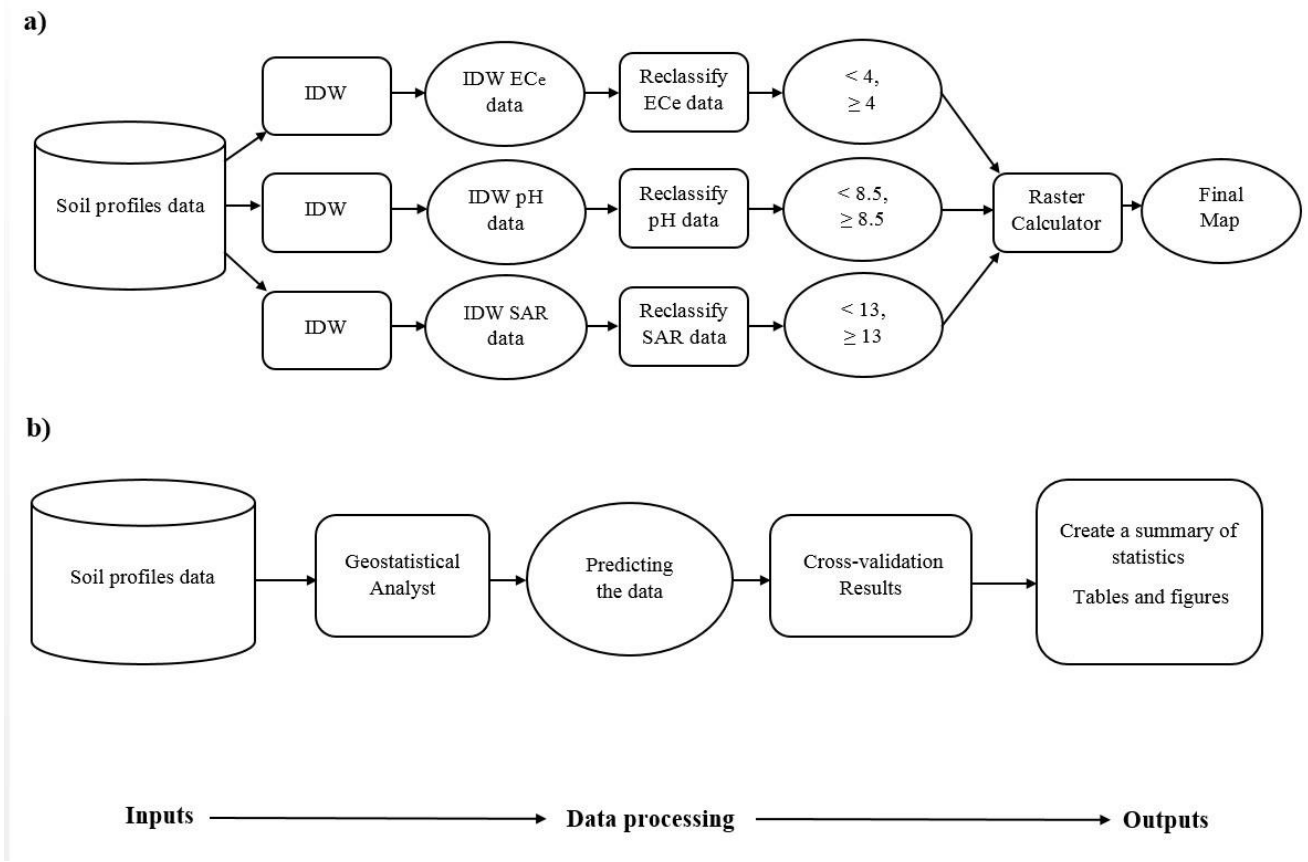

Figure 2. Flow diagram of the models created in ArcGIS Model Builder: a) Processing of the data, and b) Cross-validation.

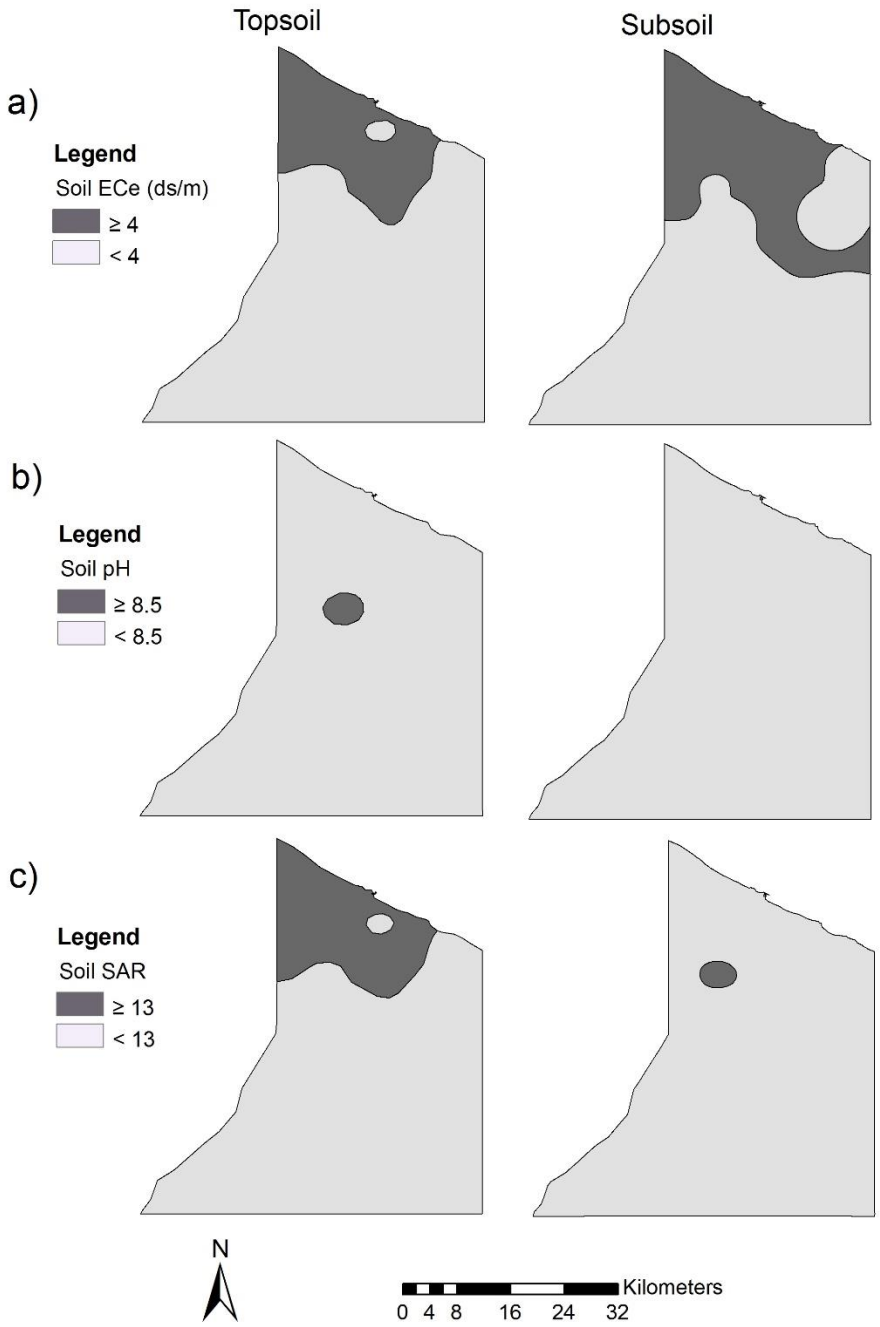

Figure 3. Maps of the topsoil (left) and subsoil (right) for: a) ECe, b) pH, and c) SAR.

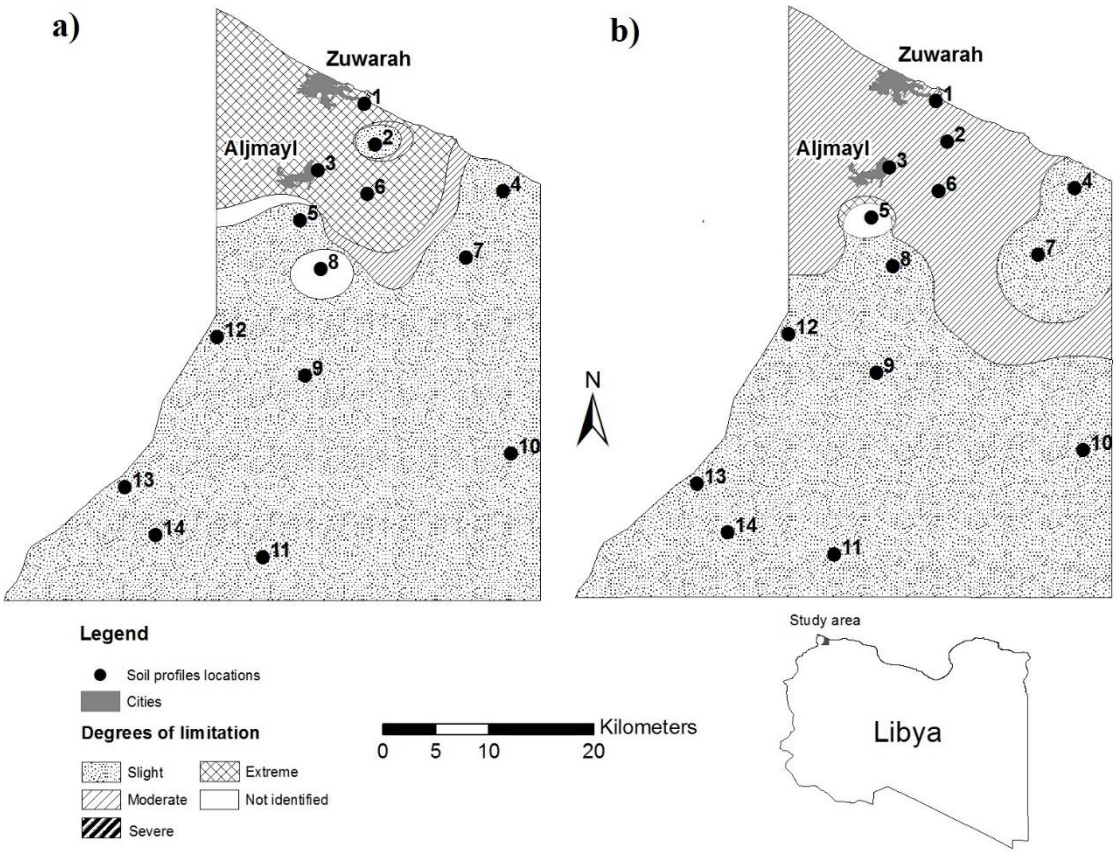

Figure 4. Salt affected soils in the study area for: a) topsoil (slight, 77%; moderate, 3%; extreme, 18%, severe, 0%, and 2% not identified area), b) subsoil (slight, 69%; moderate, 29%; extreme, 1%, severe, 0%, and 1% not identified area

CHAPTER FOUR

GEOSPATIAL ANALYSIS OF LAND USE CHANGE IN THE SAVANNAH RIVER BASIN USING GOOGLE EARTH ENGINE

This chapter is based on:

Zurqani, H.A., Post, C.J., Mikhailova, E.A., Schlautman, M.A. and Sharp, J.L., 2018. Geospatial analysis of land use change in the Savannah River Basin using Google Earth Engine. Int J Appl Earth Obs Geoinf. 69, pp.175-185.

Abstract

Climate and land use/cover change are among the most pervasive issues facing the Southeastern United States, including the Savannah River basin in South Carolina and Georgia. Land use directly affects the natural environment across the Savannah River basin and it is important to analyze these impacts. The objectives of this study are to: 1) determine the classes and the distribution of land cover in the Savannah River basin; 2) identify the spatial and the temporal change of the land cover that occurs as a consequence of land use change in the area; and 3) discuss the potential effects of land use change in the Savannah River basin. The land cover maps were produced using random forest supervised classification at four time periods for a total of thirteen common land cover classes with overall accuracy assessments of 79.18% (1999), 79.41% (2005), 76.04% (2009), and 76.11% (2015). The major land use change observed was due to the deforestation and reforestation of forest areas during the entire study period. The change detection results using the normalized difference vegetation index (NDVI) indicated that the proportion areas of the deforestation were 5.93% (1999–2005), 4.63% (2005–2009), and 3.76% (2009–2015), while the proportion areas of the reforestation

were 1.57% (1999–2005), 0.44% (2005–2009), and 1.53% (2009–2015). These results not only indicate land use change, but also demonstrate the advantage of utilizing Google Earth Engine and the public archive database in its platform to track and monitor this change over time.

Keywords: Geospatial analysis; Google earth engine (GEE); Land cover; Landsat; Remote sensing; Stream; Supervised classification; Random forest; watershed

Introduction

Land use/cover change detection can identify potential environmental events associated with rapid urbanization, forest conversion, and agricultural expansion (Drummond and Loveland, 2010; Agaton et al., 2016). Land use change is an indicator of the human footprint which can cause a loss of biodiversity and land degradation (Butt et al., 2015). Assessment and monitoring of land use change are essential for setting up integrated land and water resources management strategies (Badjana et al., 2015; Zhang et al., 2016).

Many studies have focused on identifying and examining the consequences of land use change over time. The influence of the land use change varies from one location to another due to geographic location and scale. Conversion of land from forested/agricultural to urban/suburban uses degraded aquatic ecosystems in the upper Piedmont physiographic region of South Carolina, with the change being particularly destructive during the actual land conversion process (Schlautman and Smink, 2008; Hur et al., 2008; Sciera et al., 2008). Another study in Heihe River Basin of Northwest China, revealed that land use change over time induced slight reductions in surface runoff, groundwater discharge, and streamflow (Zhang et al., 2016).

Forests have been recognized for their environmental benefits, such as water and forest product supply (Sun and Vose, 2016). For example, forests improve stream quality and watershed health by reducing the amount of stormwater runoff and pollutants that reach local waters (Schlautman and Smink, 2008; Hur et al., 2008; Sciera et al., 2008).

Over half of the water supply in the U.S. flows from forest lands (Brown et al., 2008; Sun and Vose, 2016).

Forest disturbance over time can be visualized and documented using current remote sensing and geospatial techniques. For example, Cohen et al. (2016) studied forest disturbance across the conterminous United States from 1985 to 2012 and reported that national rates of disturbance varied between 1.5% and 4.5% of the forest area per year and were primarily affected by the forest harvest cycle in heavily forested regions. Huang et al. (2010) identified stand clearing disturbance events (harvest, fire, and urban development) by using an automated algorithm based on Landsat time series. Kennedy et al. (2010) conducted a study of forest disturbance in the U.S. Pacific Northwest utilizing the yearly Landsat time series with a temporal segmentation algorithm (LandTrendr algorithm) to capture abrupt disturbance events (e.g., fire and harvest). Chen et al. (2006) studied the effect of the land cover change on terrestrial carbon dynamics in the Southern United States using annual land cover data from 1860 to 2003 and a spatially explicit process-based biogeochemical model which indicated that the primary pattern of land cover change in the area was from forests to agricultural land use.

The Savannah River basin in the Southeast region of the U.S. has been experiencing environmental change from anthropocentric activities (Twumasi and Merem, 2008; Merem et al., 2015). These changes have been documented in the Savannah River Basin Management Plan for the Georgia portion of the Savannah River basin using satellite imagery and high-altitude aerial photography (The Georgia Department of Natural Resources, 2001). Twumasi and Merem (2008) studied the

environmental change in the Savannah River basin and reported a decline in water bodies, vegetation, loss of harvested cropland, and farms. Merem et al. (2015) assessed the status of the environmental change in the Lower Savannah watershed in Georgia and South Carolina using temporal-spatial and environmental analysis and reported change in farm land use. Zhu et al. (2012) used a change detection algorithm to monitor forest disturbance at a high temporal frequency for the Savannah River site using Landsat 7 images.

There are various techniques used in analyzing land use/cover changes. Remotely sensed data holds an advantage in monitoring the detection of land cover change because of the large spatial coverage, high time resolution, and wide availability (Kennedy et al., 2009; Schneider, 2012; Vittek et al., 2014; Hu et al., 2016). Remote sensing has long been used for mapping and monitoring land use/land cover change over time (Skole and Tucker, 1993; Yang and Lo, 2002; Vittek et al., 2014; Huang et al., 2017). Despite the complications due to atmospheric disturbances, remote sensing can be used to identify and monitor land cover changes using multi-temporal satellite data and to study the relationship between the human influence on land cover and its consequences on the environment over time (Richter and Schläpfer, 2002; Butt et al., 2015).

In December 2010, Google launched a new technology named Google Earth Engine (GEE) (U.S. Geological Survey, 2010). This geospatial analysis platform made more than forty years of satellite imagery available online so that the scientists and researchers could analyze real-time changes to the Earth's surface (Houseman et al., 2015). Google Earth Engine has millions of servers around the world and has enabled the

scientific community to analyze trillions of images using parallel processing (Dong et al., 2016).

The present study utilizes the advantage of the new geospatial technology of GEE and the historical record of Landsat satellite data to investigate the land use change within the Savannah River basin located in the southeastern United States. The specific objectives of this study were to: 1) determine the classes and the distribution of land cover in the Savannah River basin; 2) identify the spatial and the temporal changes of land cover that occurred as a consequence of land use change in the area; and 3) discuss the potential impacts of land use change in the Savannah River basin.

Materials and Methods

Study area

The Savannah River basin, designated by the U.S. Geological Survey (USGS) as a six-digit hydrologic unit code (HUC 030601), defines most of the boundary between Georgia and South Carolina, and has a small portion of its headwaters North Carolina (Cooke, 1936; Twumasi and Merem, 2008) (Fig. 1). The basin covers approximately 28,000 square kilometers (Twumasi and Merem, 2008). The Savannah River itself begins at the confluence of the Seneca and Tugaloo Rivers and flows southeast to the Atlantic Ocean (Anderson, 1993). There is a variety of different land covers present in the Savannah River basin with a large area along the river covered by deciduous forest and

wetland (Zhu et al., 2012). Most of the study area is covered by evergreen forest and agriculture (Zhu et al., 2012). The modern-day Savannah River basin not only provides benefits such as hydropower generation, recreation, and flood protection (Lettenmaier et al., 1999), but it also provides a number of other important ecosystems services like the provision of wildlife habitat, recreational space, and the agricultural benefits (Anderson, 1993; U.S. Army Corps of Engineers, 2017). There are three major water reservoirs in the region: Lake Hartwell, Richard B. Russell Lake, and J. Strom Thurmond Lake, which are used for fish and wildlife management, hydropower, recreation, water quality, and water supply (Lattenmaier et al., 1999). The Thurmond Reservoir was used to cool the three nuclear reactor plants, but since their termination in 1990 the reservoir is mostly used for withdrawals for municipal, industrial, and agricultural use (Lettenmaier et al., 1999).

The basin is divided into three distinct regions: Blue Ridge province, Piedmont province, and Coastal Plain province (The Georgia Department of Natural Resources, 2001; Twumasi and Merem, 2008). The physiography of the area is the same as most of the Southeast U.S. and shows evidence of mountain formation in the Appalachian Mountains, as well as rising and declining sea levels in the coastal plain over geologic time (The Georgia Department of Natural Resources, 2001).

The climate of the Savannah River basin is divided into two regions: the coastal plain and the mountains. The coastal plain experiences hot summers and mild winters while the mountains experience mild summers and cold winters. The average annual temperature for the entire basin is 18 ° Celsius (The Georgia Department of Natural Resources, 2001). The average annual precipitation ranges from 1000 to 2000 mm per

year coming mostly from rainfall with a small percentage coming from snowfall and snowmelt from the mountains in the upper basin (The Georgia Department of Natural Resources, 2001).

Data and methods

The land use change detection technique used in this study requires image preprocessing and normalization, the reference dataset, land cover classification, and derived change and no change detection layers. The land use change detection technique was applied and evaluated by developing code in the GEE platform using a supervised classifier algorithm and Landsat time series subsequently for each chosen year (Appendix E). High-resolution aerial imagery, available in GEE, was used as a reference layer for training and validating the classifications. Comparisons were made between the classified images for each study year to find locations where land cover changed. Subsequent analysis identified changed areas where deforestation and reforestation occurred. The general procedures are summarized in the flowchart illustrated in Fig. 2. In this figure, image preprocessing, land cover categorizing, and image classification are shown as step 1, and detecting land use change is shown in step 2.

Image preprocessing

Google Earth Engine facilitates a fast analysis platform by using Google's computing infrastructure. Pre-processed Landsat imagery available through GEE was used to assess land use/land cover change across the study area. Google Earth Engine

provides online access to archived Landsat data as a collection of the USGS (Huang et al., 2017) (Table 1). All the Landsat data processing was conducted using the cloud-computing technology in the GEE platform (https://earthengine.google.org/). Landsat imagery scenes were used in this study for the years 1999, 2005, 2009, and 2015 (Table 1; Fig. 2) and were selected based on availability of high resolution aerial imagery for the study area in GEE. Simultaneously, two images were chosen for each year: summer season (June 01-July 31) and winter season (December 01-January 31) to enhance the reproducibility of the classification (Seto et al., 2002; Laborte et al., 2010; Schmidt et al., 2016). An object-based algorithm called Fmask (Function of mask) was applied to the selected Landsat scenes (i.e. single dates) to create clear observations of cloud- and cloud-shadow- free images by selecting the best cloud-free pixel (Zhu and Woodcock, 2012). Data normalization can reduce image noise and classification errors when using multi-sensor and multi-scene images (Yang and Lo, 2002). When using multi-sensor and multi-scene images it is important to normalize the data to reduce the noise resulting from sensor differences (Yang and Lo, 2002). The Normalized Difference Vegetation Index (NDVI) (Tucker, 1979; Kennedy et al., 2010), Normalized Difference Built Index (NDBI) (Xu, 2007), Modified Normalized Difference Water Index (MNDWI) (Xu, 2007; Rokni et al., 2014), and the Tasseled Cap (TC) transformations, which produce components representing brightness, greenness, wetness (Crist, 1985; Baig et al., 2014) were performed for each image using the at-sensor reflectance values and stacked for later classification. The topographic data USGS digital elevation model (DEM) was used

to distinguish between the wetlands and another type of land cover classes in a forested watershed (Sader et al., 1995; Margono et al., 2014; Jones, 2015).

Land cover categories and reference data

Classifying the heterogeneous landscape of the Savannah River basin is a challenging task (Twumasi and Merem, 2008). The heterogeneous landscape makes it possible to identify 13 land cover classes across the study area using the National Land Cover Database (NLCD) maps and description (Wickham et al., 2013), and the high-resolution imagery National Agriculture Imagery Program (NAIP) (1-m resolution) as a reference. The identified classes were 1) open water with rivers, lakes and standing water bodies, 2) low intensity urban with paved roads, concrete, and warehouses, 3) high intensity urban with densely populated areas, 4) barren land, 5) deciduous forest, 6) evergreen forest, 7) mixed forest, 8) shrub/scrub, 9) grassland/herbaceous, 10) pasture/hay, 11) cultivated crops, 12) woody wetlands, and 13) emergent herbaceous wetlands.

The reference dataset is an important consideration to the accuracy of remotely sensed data (Congalton, 1991). More than 1100 reference points were delineated for each these years 1999, 2005, 2009, and 2015, respectively, based on the availability of high-resolution imagery (NAIP) (1-m resolution) with a consideration of no less than 50 reference points per land cover category. Each point was buffered by 30 m by 30 m to enhance the classification results and ensure an objective identification of the reference data and the Landsat imagery data. A training data set that consisted of 70% randomly

selected observation was created; the remaining 30% of the observations were used in the validation data set. (Rodriguez-Galiano et al., 2012). The training dataset was used to improve the supervised classifier algorithm, while the validation dataset was used in accuracy assessment of the produced land cover classification maps.

Image classification and accuracy assessments

An extensive variety of classification algorithms have been used to map the changes in land cover/land use from remotely sensed data (Lam, 2008; Butt et al., 2015). Supervised machine learning classifiers, such as Classification and Regression Trees (CART) and Random Forest (RF), are progressively used to classify remotely sensed data (Wingate et al., 2016). The RF classifier has been effective in the classification accuracy even when applied to analyze data with stronger noise (Breiman, 2001; Tian et al., 2016). For example, Schmidt et al. (2016) compared four classification algorithms for a large area of cropping activity with the same training data and RF classifier algorithm to perform the best result. In this study, RF classifier algorithm was applied in GEE platform to obtain the land cover classification maps for each chosen year. Ensembles of 500 trees were grown using the training dataset (Breiman, 2001). The RF is an ensemble classification algorithm, which uses bootstrap aggregating or "bagging" to generate an ensemble of classification (using multiple decision trees) each tree trains on a certain subset of the entire training data (Waske and Braun, 2009). Random Forest methods are not sensitive to noise or over classifying (Gislason et al., 2006). The prediction model of the RF classifier only requires two parameters to be identified: the number of

classification trees desired, and the number of prediction variables, used in each node to make the tree grow (Rodriguez-Galiano et al., 2012).

Accuracy assessments are useful and effective techniques to determine how well the classification process accomplished the task of studies (Congalton, 1991; Sader et al., 1995; Tsutsumida and Comber, 2015). The produced land cover classification maps were validated using the validation dataset obtained from 1/3 of the reference locations. Following the previous studies (Congalton, 1991; Sader et al., 1995; Tsutsumida and Comber, 2015) a confusion matrix of land cover maps were calculated to evaluate the accuracy of the results using producer's accuracy, user's accuracy, F1 score (Deus, 2016), and Kappa statistics (Congalton and Green, 2009) (Table 2).

Land use change detection

Change detection analysis designates differences between images of the same scene at different times. The land cover classification images of the different dates were also used to calculate the area of different land cover classes and observe the changes that are taking place at that time. The land cover change areas are illustrated using mosaic plot methods to provide a visual representation of statistical surprising land use losses and gains (Comber et al., 2016). The mosaic plot provides a statistical summary of losses and gains over time. To detect one kind of land use change such as forest change, a single change index with a fixed threshold is sufficient (Zhu et al., 2012). The threshold values for defining change may also be different for different kinds of land use change (Zhu et al., 2012). Indeed, the trees can grow rapidly after a harvest and become spectrally

inseparable from the undisturbed forest in just 4–6 years, especially in the southeastern U.S (Huang et al., 2010). The change detection for forest management in the area was identified by image difference technique. The multi-date differencing NDVI bands were used to determine the change in each pixel by subtracting NDVI bands for different years. Pixels with change will be flagged as “probable change” (Zhu et al., 2012). The change detection approach was applied in four intervals: 1999–2005, 2005–2009, 2009–2015, and 1999–2015. This approach provides “from–to” change information and the type of change that has occurred can be easily calculated and mapped (Yuan et al., 2005). Optimal results obtained for the deforestation area were with threshold values of (0.05), and optimal results obtained for the reforestation area were with threshold values of (0.175). In this process, the open water areas were carefully masked out using MNDWI due to the similarity spectral with some of the growing trees area. A random stratified sample design was used for validating the change detection accuracy. A total of 500 reference pixels were selected, in which 250 pixels for the deforestation area and 250 pixels for the reforestation area (Fig. 2).

Results

Land use change and distribution

The land cover classification maps were produced using random forest supervised classification for the years 1999, 2005, 2009, and 2015 in a total of thirteen common land cover categories (Figs. 3 and 4). The individual class area for the four years is summarized in Table 3. The overall accuracies were 79.18% (1999), 79.41% (2005), 76.04% (2009), and 76.11% (2015), respectively (Table 2). It is likely that classification accuracy was reduced by the variation in availability of high-resolution imagery from the National Agriculture Imagery Program (NAIP) that was not always available for the same time period as the Landsat scenes.

Over the whole study period 1999–2015, approximately 51.70% of the total study area remained unchanged, while 48.30% changed. The urban areas and infrastructure expansion were continuously increasing over time. The barren land area declined by 215.23 km2 (0.78% of the study area) between 1999 and 2005, and this area increased by 84.49 km2, (0.31%) between 2005 and 2009. Barren land area experienced substantial change between 2009 and 2015 with an increase of 468.34 km2 (1.68%). Water bodies showed decrease in the first interval between 1999 and 2005 (by 24.89 km2 or 0.1%), increase in the second interval between 2005 and 2009 (by 14.13 km2 or 0.05%), and a decrease in the third interval between 2009 and 2015 (by 57.13 km2 or 0.21%). Over the whole study period between 1999 and 2015, the water areas declined by 67.86 km2 (0.25% of the study area). The wetlands areas experienced a substantial change in the

first interval between 1999 and 2005 where woody wetlands and emergent herbaceous wetlands increased by 403.15 km2 (1.45%), and 134.10 km2 (0.48%), respectively. However, the change appears to be insubstantial at all other intervals (Table 3).

The vegetation cover shows variable change throughout the study period. The percentage change, as well as the loss and gain of all land cover classes, is shown in Fig. 5. For the time interval 1999–2005, approximately 59.35% of the total area remained unchanged, while 40.65% changed. The forest areas of evergreen, deciduous, and mixed forest were experiencing the highest decline while the other classes which included shrub/scrub, grassland/herbaceous, pasture/hay, cultivated crops, and woody wetlands were increasing (Table 3). In the time interval 2005–2009, the unchanged area was about 61.79% of the total area, while 38.21% of the area changed. The forest areas of the evergreen and deciduous increased, while the mixed forest, shrub/scrub, grassland/herbaceous, and pasture/hay decreased, and with no substantial change appeared in the other land cover classes (Table 3). In the time interval 2009–2015, about 58.33% of the total area remained unchanged, while 41.67% changed. The areas of the deciduous and mixed forests, and cultivated crops increased, while the evergreen forest, shrub/scrub, grassland/herbaceous, and pasture/hay decreased. For the whole study area, the predominant land cover transitions at each time interval were changes from forests areas to shrub/scrub, grassland/herbaceous, and cultivated crops, and vice versa.

The mosaic plot in Fig. 5 represents a statistical summary of losses and gains for four-time intervals: 1999–2005, 2005–2009, 2009–2015, and 1999–2015. The plot indicates that gains of deciduous and evergreen forests are substantially greater than

would be expected in all-time intervals except in the first interval where it showed a small gain of evergreen forest between the year 1999 and 2005. The mosaic plot also showed smaller gains and losses of shrub/scrub and grassland/herbaceous in all time intervals except in the first interval of the grassland/herbaceous where the gain was greater than would be expected between the year 1999 and 2005. Detailed comparisons of specific losses and gains for individual classes of land use for each time interval are shown in Appendix A, 2, 3, and 4.

Forest management and change detection

During the study period, the main land cover change occurred in forest areas. The change detection results indicate that the deforestation area between 1999 and 2005 was 1653.50 km2 (5.93%), while the reforestation area was 436.67.61 km2 (1.57%). Deforestation from 2005 to 2009 accounted for 1229.22 km2 (4.63%) of the study area, while the 123.50 km2 (0.44%) was reforested. From 2009–2015, 1047.10 km2 (3.76%) was deforested, and 426.40 km2 (1.53%) was reforested. Over the 16 year study period (1999–2015), 1235.93 km2 (4.43%) was deforested, and a larger area was reforested (1395.69 km2; 5.00%) (Table 4).

An area of approximately 370.35 km2 that was deforested in 1999–2005 was identified as being a new reforestation area in 2005–2009, and about 540.90 km2 of the deforestation area in 2005–2009 was identified as a new reforestation area in 2009–2015. The overall accuracy of the study for the deforestation and reforestation was 67.60% and 70.80% for the first interval (1999–2005), 72.40% and 66.80% for the second interval

(2005–2009), 71.20% and 65.20% for the third interval (2009–2015), and 68.00% and 71.60% for the entire study period (1999–2015), respectively (Table 4).

Discussion

Advantages and limitations of the proposed land cover classification method

The proposed land cover classification method uses the Random Forest (RF) supervised classification algorithm using a number of indices and topographic data within the GEE platform (Fig. 2). The Random Forest (RF) algorithm provides flexibility in the modeling process for inclusion of disparate data types (Breiman 2001) and it accurately classifies the heterogeneous land cover in the Savannah River basin. The method also utilized NDVI change detection (Huang et al., 2017; Johansen et al., 2015; Kennedy et al., 2010; Zhu et al., 2012) which helped identify the deforestation and reforestation activities and explained the correlation between the shrub/scrub and grassland/herbaceous and forests areas.

The GEE platform enables high-speed analysis using advanced processing tools for large regions and large datasets, without having to find and download remote sensing data for desktop processing. All datasets and algorithms in GEE are available free for non-commercial use. Google Earth Engine has millions of servers around the world and has enabled the scientific community to analyze trillions of images using parallel processing (Dong et al., 2016). It also allows the use of algorithms that combine data from multiple sensors and years/seasons and/or models. Google Earth Engine has

routines that can combine images (for a particular date range) to find the best cloud-free pixel which when re-assembled creates cloud-free images for a particular region (Gorelick et al., 2017). This method can be used to accurately track land cover change on a monthly basis as the analysis can easily be re-run as new remote sensing layers are automatically acquired by GEE which will help identify the wide range of disturbance that occurs in the earth's surface over time. For example, deforestation, urban growth, agriculture expansion, wetland loss, and quantifying changes in the world's forests (Alonso et al., 2016; Dong et al., 2016; Goldblatt et al., 2016; Hansen et al., 2013; Johansen et al., 2015).

The limitation of the use of this approach can include the lack of the high-resolution aerial imagery to act as a reference for the classification results (although it is possible to upload additional datasets to include in the analysis). Also, the limited availability of other algorithms in GEE which may improve the classification accuracy, for example, image segmentation and object-based image classification options are limited or in testing phases (Camara et al., 2016). Furthermore, processing power can be limited by the GEE system, which can cause errors in analysis over large spatial areas or with large computational complexity due to per-worker memory limitations (Gorelick et al., 2017).

Implications of land cover change analysis for the Savannah river basin

Based on the classification results, agriculture activities have resulted in a gradual spread of land cover classes in the form of loss and gains. A major land use change in the

study area was a result of urbanization, increased agricultural use and forest management. Though the potential land use change took place throughout the basin, most of the direct influence on the study area appeared to be near the lakes and the tributary waters. Therefore, the analysis shows a repeated dispersion of the loss and gain in land use classes within the Savannah River basin (Fig. 3). Nash and Chaloud (2011) indicated that the agriculture activities, erodible soils and urbanization negatively affect the biotic condition in the Savannah River basin. The U.S. Environmental Protection Agency (2001) reported that agriculture activities in the area have a higher potential for soil erosion due to the steep slopes in highly or moderately erodible soils.

Although the spatial extent of urban areas is small compared to the other major land cover classes, urban areas can be disproportionally change the environment when compared to other land use classes. Comparison of the land cover classification results over the entire study period indicates a clear increase in the urban areas coupled with a decrease in the shrub/scrub and grassland/herbaceous and some forests area (Table 3). The accelerated increase of the urbanization and the conversion of the vegetation cover, including farmland and forests to urban developments, reduce the lands that are available for food and timber production (Wu, 2008). In the Savannah River basin, the conversion of the vegetation cover, including the urban growth, agriculture expansion, and deforestation and reforestation take place throughout the basin, especially near the lakes and tributary waters in the middle and lower Savannah Basin. The continuous change of the land use such as the conversion of forest areas to other types of the land cover and vice versa can significantly lead to increasing threats to the environmental systems of the

region. Lubowski et al. (2006) pointed that soil erosion and degradation coupled with intensive agriculture activities and deforestation are reducing the quality of land resources and future agricultural productivity.

Forests have dominated the central area of the Savannah River. The Georgia Department of Natural Resources (2001) reported that the forestry is a major part of the economy within the basin, and the forest industry output for 1997 grew to approximately $19.5 billion statewide. Changes in the forests' area were illustrated as where the deforestation and the reforestation occur using the Normalized Difference Vegetation Index (NDVI) revealed evidence supporting the case of this study. A substantial change was observed by tracking the deforestation area in 1999. The result shows an evidence of the forest management over time in the region–for example, the evergreen forest coverage was about 53% of this area in 1999, and this area decreased to 8% 2005, and then increased to 26% in 2009 and to 32% in 2015, while the grassland/herbaceous increased from 4% in 1999 to 30% in 2005 and then decreased to 17% in 2009 and 9% in 2015 (Fig. 6). Carlson (2004) used a combination of satellite image classification with an urban growth model and found that woodland regrowth is predicted to occur in grass/scrub non-forested areas, which is similar to what was found in the current study.

Potential applications and limitations of the land cover classification method to other areas

The proposed method is more applicable to the regions that have the land cover types dominated by forests. The results show that forests areas and wetlands had high

classification accuracies with this method (Fig. 6). Using this approach in GEE allows the comparison of multiple indices used in the classification process by showing the classification accuracy at the same time as performing the image classification. Recently, multiple land cover change monitoring studies have used the archived Landsat data in GEE to detect the global forest change, monitoring woody vegetation clearing and identifying mangrove forest cover change over time (Hansen et al., 2013; Housman et al., 2015; Johansen et al., 2015; Giri et al., 2015).

The primary limitation of this method is the requirement of having high-resolution aerial imagery to obtain the reference data for the classification and the validation process, which is not available for all regions in the world. New availability of high-resolution satellite imagery in GEE may solve this issue in the future. Google Earth Engine can be used to classify images for any area in the world to detect the land use change if a source of high-resolution aerial or satellite imagery are available.

Conclusions

The availability of the historical data of Landsat imagery as well as the new geospatial Google Earth Engine technology represent a major improvement for monitoring and evaluating land use change over large geographic regions. This study successfully develops a regional scale analysis and determines the classes and the distribution of land cover in Savannah River basin, and identified the spatial and the temporal change of the land cover that occurred as a consequence of land use change

over the past 16 years in the Savannah River basin. Land use change was observed to be dominant in the forest areas during all intervals of the study period.

All the classification and the validation processes in this study were accomplished using GEE cloud computation by processing and comparing multiple Landsat scenes over the study period between 1999 and 2015. The limitation of the Random Forest classifier and the change detection approaches is the requirement of the reference dataset which requires high-resolution imagery. Google Earth Engine platform makes the historical data Landsat imagery available to the users, but the challenge is finding the source to the reference dataset especially before the year 2003. In future studies, continuous monitoring of the land cover may provide management strategies that are able to react to and mitigate the environmental consequences of this change.

References

Ally, M. Foundations of educational theory for online learning. 2008. Theory and Practice of Online Learning, 2nd Edition: 15-44. AU Press, Athabasca University, Edmonton, AB (Canada).

Agaton, M., Setiawan, Y., Effendi, H., 2016. Land use/land cover change detection in an urban watershed: A case study of upper Citarum Watershed West Java Province, Indonesia. Procedia Environ. Sci. 33, 654–660.

Alonso, A., Muñoz-Carpena, R., Kennedy, R.E., Murcia, C., 2016. Wetland landscape spatio-temporal degradation dynamics using the new Google Earth Engine cloudbased platform: Opportunities for non-specialists in remote sensing. Trans. ASABE 59 (5), 1333–1344.

Anderson, M.C., 1993. A Watershed Protection Project: The Savannah River. Environmental Protection Agency. Savannah River Basin Watershed Project.

Badjana, H.M., Helmschrot, J., Selsam, P., Wala, K., Flügel, W.A., Afouda, A., Akpagana, K., 2015. Land cover changes assessment using object-based image analysis in theBinah River watershed (Togo and Benin). Earth Space Sci. 2 (10), 403–416.

Baig, M.H.A., Zhang, L., Shuai, T., Tong, Q., 2014. Derivation of a tasselled cap transformation based on Landsat 8 at-satellite reflectance. Remote Sens. Lett. 5, 423–431.

Breiman, L., 2001. Random forests. Mach. Learn. 45 (1), 5–32.

Brown, T.C., Hobbins, M.T., Ramirez, J.A., 2008. Spatial distribution of water supply in the coterminous United States. J. Am. Water Res. Assoc. 44 (6), 1474–1487.

Butt, A., Shabbir, R., Ahmad, S.S., Aziz, N., 2015. Land use change mapping and analysis using Remote Sensing and GIS: A case study of Simly watershed, Islamabad, Pakistan. Egypt. J. Rem. Sens. Space Sci. 18, 251–259.

Camara, G., Assis, L.F., Ribeiro, G., Ferreira, K.R., Llapa, E., Vinhas, L., 2016. Big earth observation data analytics: Matching requirements to system architectures. In Proceedings of the 5th ACM SIGSPATIAL International Workshop on Analytics for Big Geospatial Data 1–6 (ACM).

Carlson, T.N., 2004. Analysis and prediction of surface runoff in an urbanizing watershed using satellite imagery. J. Am. Water Res. Assoc. 40 (4), 1087–1098.

Chen, H., Tian, H., Liu, M., Melillo, J., Pan, S., Zhang, C., 2006. Effect of land-cover change on terrestrial carbon dynamics in the southern United States. J. Environ. Qual. 35 (4), 1533–1547.

Cohen, W.B., Yang, Z., Stehman, S.V., Schroeder, T.A., Bell, D.M., Masek, J.G., Huang, C., Meigs, G.W., 2016. Forest disturbance across the conterminous United States from 1985 to 2012: The emerging dominance of forest decline. For. Ecol. Manage. 360, 242–252.

Comber, A., Balzter, H., Cole, B., Fisher, P., Johnson, S., Ogutu, B., 2016. Methods to quantify regional differences in land cover change. Remote Sens. 8 (3), 176.

Congalton, R.G., Green, K., 2009. Assessing the Accuracy of Remotely Sensed Data: Principles and Practices, 2nd ed. CRC Press, Boca Raton, FL.

Congalton, R.G., 1991. A review of assessing the accuracy of classifications of remotely sensed data. Remote Sens. Environ. 37 (1), 35–46.

Cooke, C.W., 1936. Geology of the coastal plain of South Carolina. US Geol. Surv. Bull. 867, 196.

Crist, E.P., 1985. A TM tasseled cap equivalent transformation for reflectance factor data. Remote Sens. Environ. 17 (3), 301–306.

Deus, D., 2016. Integration of ALOS PALSAR and landsat data for land cover and forest mapping in northern Tanzania. Land 5 (4), 43.

Dong, J., Xiao, X., Menarguez, M.A., Zhang, G., Qin, Y., Thau, D., Biradar, C., Moore, B., 2016. Mapping paddy rice planting area in northeastern Asia with Landsat 8 images, phenology-based algorithm and Google Earth Engine. Remote Sens. Environ. 185, 142–154.

Drummond, M.A., Loveland, T.R., 2010. Land-use pressure and a transition to forest-cover loss in the eastern United States. BioScience 60, 286–298.

Giri, C., Long, J., Abbas, S., Murali, R.M., Qamer, F.M., Pengra, B., Thau, D., 2015. Distribution and dynamics of mangrove forests of South Asia. J. Environ. Manage. 148, 101–111.

Gislason, P.O., Benediktsson, J.A., Sveinsson, J.R., 2006. Random forests for land cover classification. Pattern Recognit. Lett. 27 (4), 294–300.

Goldblatt, R., You, W., Hanson, G., Khandelwal, A.K., 2016. Detecting the boundaries of urban areas in india: A dataset for pixel-based image classification in Google Earth Engine. Remote Sens. 8 (8), 634.

Gorelick, N., Hancher, M., Dixon, M., Ilyushchenko, S., Thau, D., Moore, R., 2017. Google Earth Engine: Planetary-scale geospatial analysis for everyone. Remote Sens. Environ. 203, 18–27.

Hansen, M.C., Potapov, P.V., Moore, R., Hancher, M., Turubanova, S.A., Tyukavina, A., Thau, D., Stehman, S.V., Goetz, S.J., Loveland, T.R., Kommareddy, A., 2013. High resolution global maps of 21st-century forest cover change. Science 342 (6160), 850–853.

Housman, I., Tanpipat, V., Biswas, T., Clark, A., Stephen, P., Maus, P., Megown, K., 2015. Monitoring Forest Change in Southeast Asia: Case Studies for USAID Lowering

Emissions in Asia's Forests. RSAC-10108-RPT1. U.S. Department of Agriculture, Forest Service, Remote Sensing Applications Center, Salt Lake City, UT, pp. 16.

Hu, T., Yang, J., Li, X., Gong, P., 2016. Mapping urban land use by using Landsat images and open social data. Remote Sens. 8, 151.

Huang, C., Goward, S.N., Masek, J.G., Thomas, N., Zhu, Z., Vogelmann, J.E., 2010. An automated approach for reconstructing recent forest disturbance history using dense Landsat time series stacks. Remote Sens. Environ. 114 (1), 183–198.

Huang, H., Chen, Y., Clinton, N., Wang, J., Wang, X., Liu, C., Gong, P., Yang, J., Bai, Y., Zheng, Y., Zhu, Z., 2017. Mapping major land cover dynamics in Beijing using all Landsat images in Google Earth Engine. Remote Sens. Environ in press.

Hur, J., Schlautman, M.A., Templeton, S.R., Karanfil, T., Post, C.J., Smink, J.A., Song, H., Goddard, M.A., Klaine, S.J., Hayes, J.C., 2008. Does current management of

storm water runoff adequately protect water resources in developing catchments? J. Soil Water Conserv. 63 (2), 77–90.

Johansen, K., Phinn, S., Taylor, M., 2015. Mapping woody vegetation clearing in Queensland, Australia from Landsat imagery using the Google Earth Engine. Remote Sensing applications. Soc. Environ. 1, 36–49.

Jones, J.W., 2015. Efficient wetland surface water detection and monitoring via Landsat: Comparison with in situ data from the Everglades Depth Estimation Network. Remote Sens. 7, 12503–12538.

Kennedy, R.E., Townsend, P.A., Gross, J.E., Cohen, W.B., Bolstad, P., Wang, Y.Q., Adams, P., 2009. Remote sensing change detection tools for natural resource managers:

Understanding concepts and tradeoffs in the design of landscape monitoring projects. Remote Sens. Environ. 113, 1382–1396.

Kennedy, R.E., Yang, Z., Cohen, W.B., 2010. Detecting trends in forest disturbance and recovery using yearly Landsat time series: 1: LandTrendr–Temporal segmentation algorithms. Remote Sens. Environ. 114 (12), 2897–2910.

Laborte, A.G., Maunahan, A.A., Hijmans, R.J., 2010. Spectral signature generalization and expansion can improve the accuracy of satellite image classification. PLOS ONE 5 (5), e10516.

Lam, N.S.N., 2008. Methodologies for mapping land cover/land use and its change. In: Liang, S. (Ed.), Advances in Land Remote Sensing. Springer, Netherlands, pp. 341–367.

Lettenmaier, D.P., Wood, A.W., Palmer, R.N., Wood, E.F., Stakhiv, E.Z., 1999. Water resources implications of global warming: A US regional perspective. Clim. Change 43 (3), 537–579.

Lubowski, R., Vesterby, M., Bucholtz, S., Baez, A., Roberts, M., 2006. Major Uses of Land in the United States 2002. Economic Information Bulletin (EIB-14). U.S. Department of Agriculture, Economic Research Service, Washington, D.C., USA.

Margono, B.A., Bwangoy, J.R.B., Potapov, P.V., Hansen, M.C., 2014. Mapping wetlands in Indonesia using Landsat and PALSAR data-sets and derived topographical indices. Geo-Spatial Inf. Sci. 17, 60–71.

Merem, E.C., Wesley, J., Nwagboso, E., Fageir, S., Nichols, S., Thomas, T., Isokpehi, P., Crisler, M., Romorno, C., 2015. Analyzing environmental issues in the lower Savannah watershed, in Georgia and South Carolina. Am. J. Environ. Eng. 5, 1–20.

Nash, M.S., Chaloud, D.J., 2011. Partial least square analyses of landscape and surface water biota associations in the Savannah River Basin. Int. Scholarly Res. Netw.

Richter, R., Schläpfer, D., 2002. Geo-atmospheric processing of airborne imaging spectrometry data Part 2. Atmospheric/topographic correction. Int. J. Remote Sens. 23, 2631–2649.

Rodriguez-Galiano, V.F., Ghimire, B., Rogan, J., Chica-Olmo, M., Rigol-Sanchez, J.P., 2012. An assessment of the effectiveness of a random forest classifier for land-cover classification. ISPRS J. Photogramm. Remote Sens. 67, 93–104.

Rokni, K., Ahmad, A., Selamat, A., Hazini, S., 2014. Water feature extraction and change detection using multitemporal Landsat imagery. Remote Sens. 6 (5), 4173–4189.

Sader, S.A., Ahl, D., Liou, W.S., 1995. Accuracy of Landsat-TM and GIS rule-based methods for forest wetland classification in Maine. Remote Sens. Environ. 53, 133–144.

Schlautman, M.A., Smink, J.A., 2008. Evaluating the collective performance of best management practices in catchments undergoing active land development. J. Soil Water Conserv. 63 (2), 54A–55A.

Schmidt, M., Pringle, M., Devadas, R., Denham, R., Tindall, D., 2016. A framework for large-area mapping of past and present cropping activity using seasonal Landsat mages and time series metrics. Remote Sens. 8 (4), 312.

Schneider, A., 2012. Monitoring land cover change in urban and peri-urban areas using dense time stacks of Landsat satellite data and a data mining approach. Remote Sens. Environ. 124, 689–704.

Sciera, K.L., Smink, J.A., Morse, J.C., Post, C.J., Pike, J.W., English, W.R., Karanfil, T., Hayes, J.C., Schlautman, M.A., Klaine, S.J., 2008. Impacts of land disturbance on aquatic ecosystem health: Quantifying the cascade of events. Integr. Environ. Asses. 4 (4), 431–442.

Seto, E., Xu, B., Liang, S., Gong, P., Wu, W., Davis, G., Qiu, D., Gu, X., Spear, R., 2002. The use of remote sensing for predictive modeling of schistosomiasis in China. Photogramm. Eng. Rem. Sens. 68, 167–174.

Skole, D., Tucker, C.J., 1993. Tropical deforestation and habitat fragmentation in the Amazon: Satellite data from 1978 to 1988. Science 260, 1905–1910.

Sun, G., Vose, J.M., 2016. Forest management challenges for sustaining water resources in the Anthropocene. Forests 7 (3), 68.

The Georgia Department of Natural Resources, 2001. Savannah River Basin Management Plan 2001. Georgia Department, of Natural Resources, Environmental Protection Division.

Tian, S., Zhang, X., Tian, J., Sun, Q., 2016. Random forest classification of wetland landcovers from multi-sensor data in the arid region of Xinjiang. China. Remote Sens. 8 (11), 954.

Tsutsumida, N., Comber, A.J., 2015. Measures of spatio-temporal accuracy for time series land cover data. Int. J. Appl. Earth Obs. Geoinf. 41, 46–55.

Tucker, C.J., 1979. Red and photographic infrared linear combinations for monitoring vegetation. Remote Sens. Environ. 8 (2), 127–150.

Twumasi, Y.A., Merem, E.C., 2008. Geospatial information systems analysis of regional nvironmental change along the Savannah river basin of Georgia. Int. J. Environ. Res. Public Health 5, 54–67.

U.S. Army Corps of Engineers, 2017. Savannah River Basin Comprehensive Study, GA & SC, Interim Study 2: Integrated Feasibility Report and Environmental Assessment for the Drought Contingency Plan Update. June 2017. pp. 128 URL [http://www.sas.usace.army.mil/Portals/61/docs/Savannah%20River%20Basin%Comprehensive%20Study%20GA%20and%20SC%20Interim%20Study%202%20

EA%20and%20Draft%20Finding%20of%20No%20Significant%20Impact%20FONSI.pdf?ver=2017-06-12-143800-793] (Accessed 27.09.2017).

U.S. Environmental Protection Agency, 2001. Savannah River Basin Landscape Analysis. Office of Research and Development Washington.

U.S. Geological Survey, 2010. Thousands of Landsat Scenes in Google's Earth Engine. URL https://landsat.usgs.gov/google-earth-engine (Accessed 02.12.2017).

Vittek, M., Brink, A., Donnay, F., Simonetti, D., Desclée, B., 2014. Land cover change monitoring using Landsat MSS/TM satellite image data over West Africa between 1975 and 1990. Remote Sens. 6, 658–676.

Waske, B., Braun, M., 2009. Classifier ensembles for land cover mapping using multitemporal SAR imagery. ISPRS J. Photogramm. Remote Sens. 64 (5), 450 457.

Wickham, J.D., Stehman, S.V., Gass, L., Dewitz, J., Fry, J.A., Wade, T.G., 2013. Accuracy assessment of NLCD 2006 land cover and impervious surface. Remote Sens. Environ. 130, 294–304.

Wingate, V.R., Phinn, S.R., Kuhn, N., Bloemertz, L., Dhanjal-Adams, K.L., 2016. Mapping decadal land cover changes in the woodlands of north eastern Namibia from 1975 to 2014 using the Landsat satellite archived data. Remote Sens. 8 (8), 681.

Wu, J., 2008. Land use changes: Economic, social, and environmental impacts. Choices 23 (4), 6–10.

Xu, H., 2007. Extraction of urban built-up land features from Landsat imagery using a thematic oriented index combination technique. Photogramm. Eng. Remote Sens. 73 (12), 1381–1391.

Yang, X., Lo, C.P., 2002. Using a time series of satellite imagery to detect land use and land cover changes in the Atlanta: Georgia metropolitan area. Int. J. Remote Sens. 23, 1775–1798.

Yuan, F., Sawaya, K.E., Loeffelholz, B.C., Bauer, M.E., 2005. Land cover classification and change analysis of the Twin Cities (Minnesota) Metropolitan Area by multitemporal Landsat remote sensing. Remote Sens. Environ. 98 (2), 317–328.

Zhang, L., Nan, Z., Xu, Y., Li, S., 2016. Hydrological impacts of land use change and climate variability in the headwater region of the Heihe River Basin, Northwest China. PloS one 11 (6), e0158394.

Zhu, Z., Woodcock, C.E., 2012. Object-based cloud and cloud shadow detection in Landsat imagery. Remote Sens. Environ. 118, 83–94.

Zhu, Z., Woodcock, C.E., Olofsson, P., 2012. Continuous monitoring of forest disturbance using all available Landsat imagery. Remote Sens. Environ. 122, 75–91.

APPENDIX A

Table 1. Data sources and descriptions.

Data Layer	Source	Spatial Resolution (meter)	Date
Watershed Boundary Dataset (WBD), Strems	U.S. Department of the Interior, U.S. Geological Survey	Scale 1:24,000	2016
Landsat 8 Surface Reflectance (SR)	Google earth engine (GEE) data provided by U.S. Geological Survey (USGS)	30	2015
Landsat 5 Surface Reflectance (SR)	Google earth engine (GEE) data provided by U.S. Geological Survey (USGS)	30	1999, 2005, and 2009
National Land Cover Database (NLCD)	Google earth engine (GEE) data provided by U.S. Geological Survey (USGS)	30	2001, 2006, and 2011
National Agriculture Imagery Program (NAIP)	Google earth engine (GEE) data provided by U.S. Department of Agriculture (USDA)	1	1999, 2005, 2009, and 2015
Digital Elevation Model (DEM)	Google earth engine (GEE) data provided by NASA / USGS / Jet Propulsion Laboratory-Caltech	30	2000

Table 2. The percentage of producer's, user's, F1 score, overall accuracy and kappa statistic for land cover classification.

No	Types	1999			2005			2009			2015		
		User's accuracy	Producer's accuracy	F1 Score	User's accuracy	Producer's accuracy	F1 Score	User's accuracy	Producer's accuracy	F1 Score	User's accuracy	Producer's accuracy	F1 Score
1	Water	100.00	89.33	94.36	100.00	100.00	100.00	98.02	100.00	99.00	100.00	91.81	95.73
2	Low intensity urban	60.29	66.13	63.08	89.36	71.18	79.24	80.00	72.00	75.79	63.15	68.57	65.75
3	High intensity urban	80.59	73.97	77.14	81.81	80.89	81.35	81.91	73.33	77.38	81.03	68.11	74.01
4	Barren Land	81.15	66.66	73.19	74.25	81.52	77.72	65.26	72.10	68.51	68.85	82.35	75.00
5	Deciduous Forest	86.74	91.91	89.25	80.57	90.69	85.33	78.73	90.62	84.26	79.70	89.62	84.37
6	Evergreen Forest	84.56	96.82	90.28	84.22	99.15	91.08	82.30	87.33	84.74	84.09	84.69	84.39
7	Mixed Forest	56.25	31.58	40.45	78.78	37.14	50.48	59.45	37.93	46.31	34.00	41.46	37.36
8	Shrub/ Scrub	57.14	61.02	59.02	59.25	51.61	55.17	38.46	21.74	27.78	52.94	41.53	46.55
9	Grassland/ Herbaceous	66.15	61.43	63.70	50.00	50.00	50.00	52.77	41.30	46.34	64.58	41.33	50.40
10	Pasture/Hay	67.06	98.28	79.72	84.48	76.56	80.33	53.08	74.13	61.86	100.00	67.44	80.55
11	Cultivated Crops	77.77	59.32	67.30	63.01	85.18	72.44	63.07	56.16	59.41	59.15	77.77	67.19
12	Woody Wetlands	72.00	62.79	67.08	68.05	47.11	55.68	90.90	76.27	82.94	71.42	70.51	70.96
13	Emergent Herbaceous Wetlands	89.83	79.10	84.12	94.66	93.42	94.04	69.84	95.65	80.73	66.04	79.45	72.13
	Overall accuracy	79.18			79.41			76.04			76.11		
	kappa Coefficient	76.25			76.82			73.13			72.80		

Table 3. The distribution of land cover classification for each chosen year.

No	Land Use classes	The coverage area for each year							
		1999		2005		2009		2015	
		Km^2	(%)	Km^2	(%)	Km^2	(%)	Km^2	(%)
1	Water	795.29	2.86	770.40	2.77	784.53	2.82	727.40	2.61
2	Low intensity urban	366.94	1.32	392.75	1.41	460.29	1.65	671.14	2.41
3	High intensity urban	50.83	0.18	73.19	0.26	59.67	0.21	86.32	0.31
4	Barren land	491.79	1.77	276.56	0.99	361.05	1.30	829.39	2.98
5	Deciduous forest	6813.04	24.46	6248.94	22.44	7289.08	26.17	6269.35	22.51
6	Evergreen forest	6120.36	21.97	4982.35	17.89	6458.72	23.19	6923.97	24.86
7	Mixed forest	2649.88	9.51	1954.73	7.02	1866.54	6.70	2750.71	9.88
8	Shrub/ Scrub	1601.70	5.75	2393.52	8.59	1324.85	4.76	1190.97	4.28
9	Grassland/ Herbaceous	2872.61	10.31	3311.55	11.89	2463.10	8.84	1525.25	5.48
10	Pasture/ Hay	2360.94	8.48	3068.34	11.02	2626.28	9.43	2494.77	8.96
11	Cultivated crops	1099.72	3.95	1213.54	4.36	1213.64	4.36	1614.86	5.80
12	Woody wetlands	1968.51	7.07	2371.66	8.52	2356.40	8.46	2164.26	7.77
13	Emergent herbaceous wetlands	660.33	2.37	794.43	2.85	587.79	2.11	603.55	2.17
	Total	27851.94	100.00	27851.96	100.00	27851.94	100.00	27851.94	100.00

Table 4. The Forest management over time.

Time	Forest management	Coverage area		Percentage of the correct and incorrect check points	
		Km^2	(%)	Correct	Incorrect
1999 - 2005	Deforestation	1653.50	(5.93)	67.60 (n=169)	32.40 (n=81)
	Reforestation	436.67	(1.57)	70.80 (n= 177)	29.20 (n=79)
2005- 2009	Deforestation	1229.22	(4.63)	72.40 (n=181)	27.60 (n=69)
	Reforestation	123.50	(0.44)	66.80 (n= 167)	33.20 (n=83)
2009- 2015	Deforestation	1047.10	(3.76)	71.20 (n=178)	28.80 (n=72)
	Reforestation	426.40	(1.53)	65.20 (n= 163)	34.80 (n=87)
1999- 2015	Deforestation	1235.93	(4.43)	68.00 (n=170)	32.00 (n=80)
	Reforestation	1395.69	(5.00)	71.60 (n=179)	28.40 (n=71)

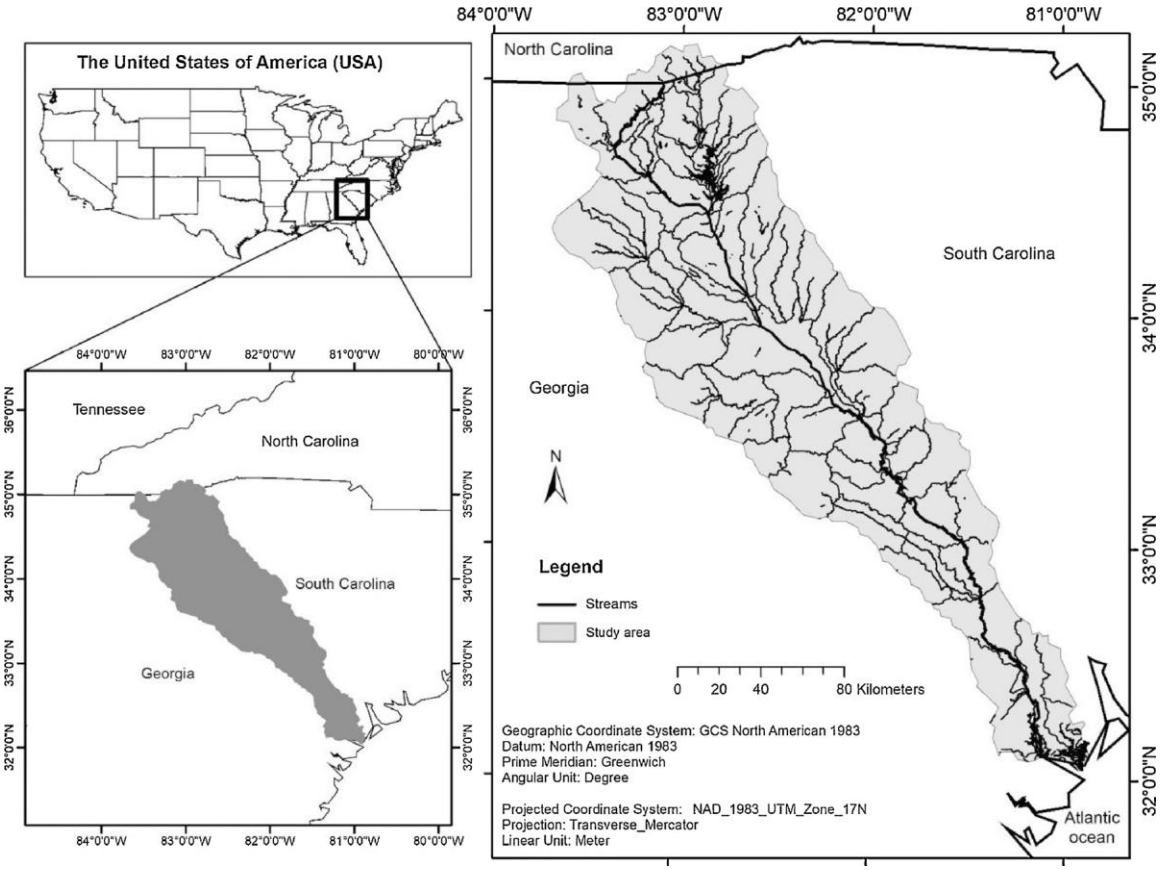

Figure 1. Location of the Savannah River Basin.

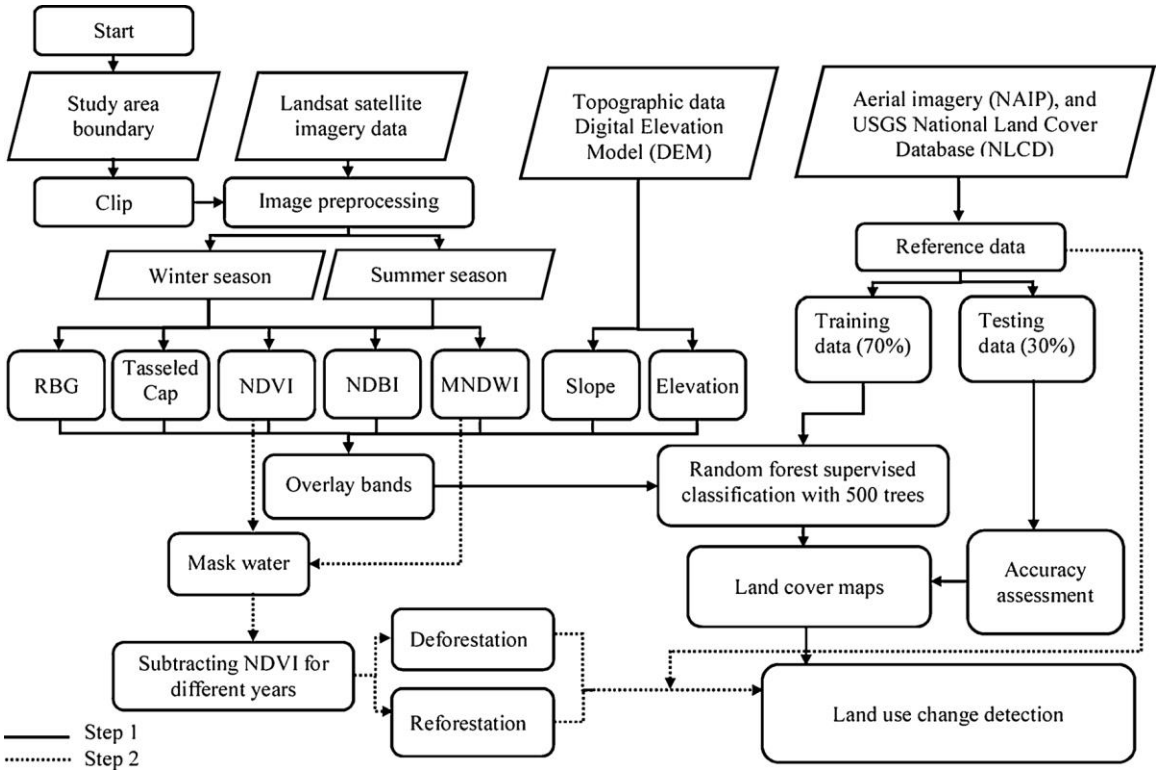

Figure 2. Flow chart of data processing. Step 1 shows the path for creating the land cover maps (methods Sections 3.1–3.3), while step 2 identifies land use change (methods Section 3.4).

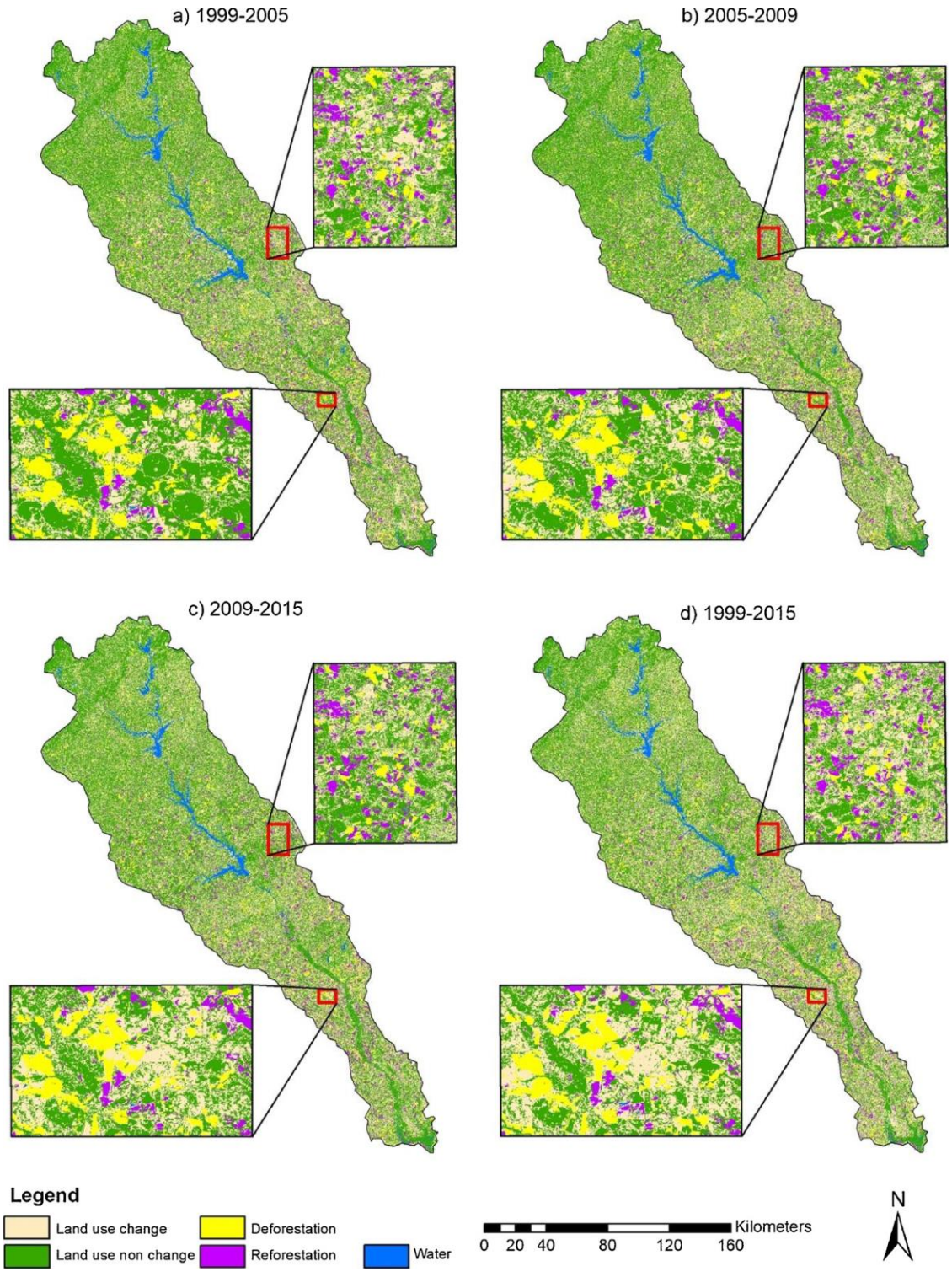

Figure 3. The distribution of land use change (including deforestation and reforestation) in the Savannah River Basin. Inset maps show land cover change for specific areas.

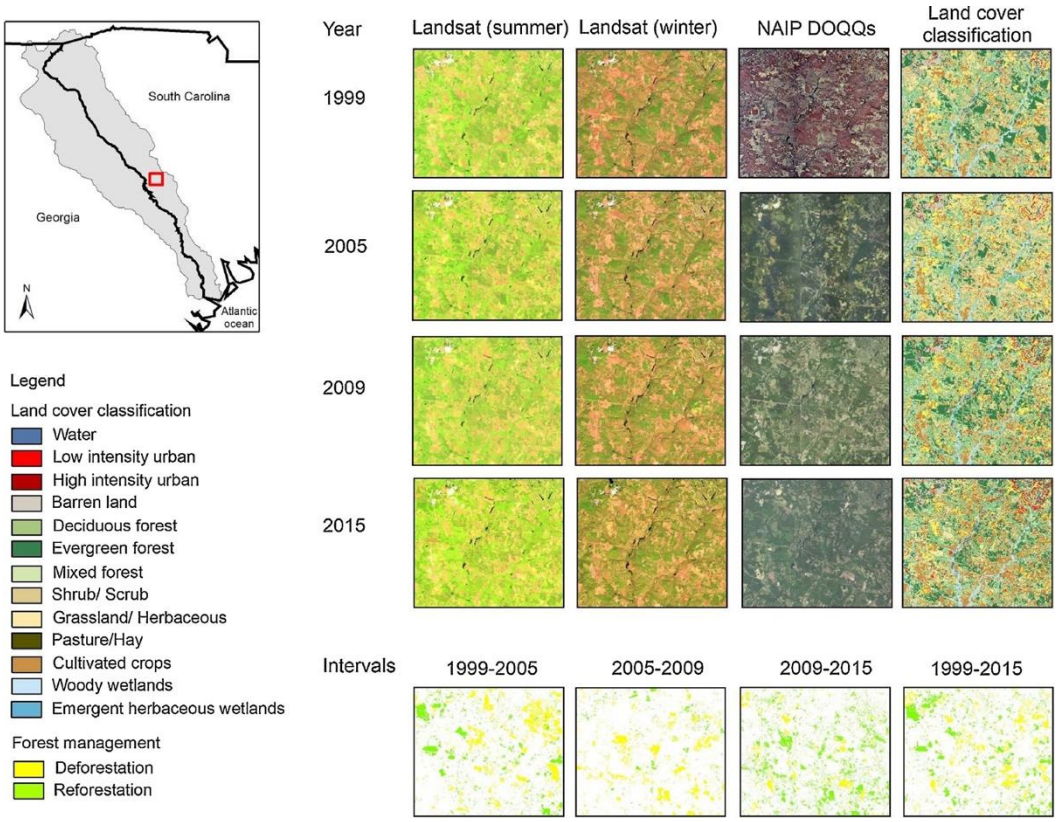

Figure 4. Landsat images in both seasons, NAIP, land cover classification, and the forest land management for the area highlighted by the red box. Land cover classification (methods Sections 3.1–3.3). Forest management intervals (methods Section 3.4).

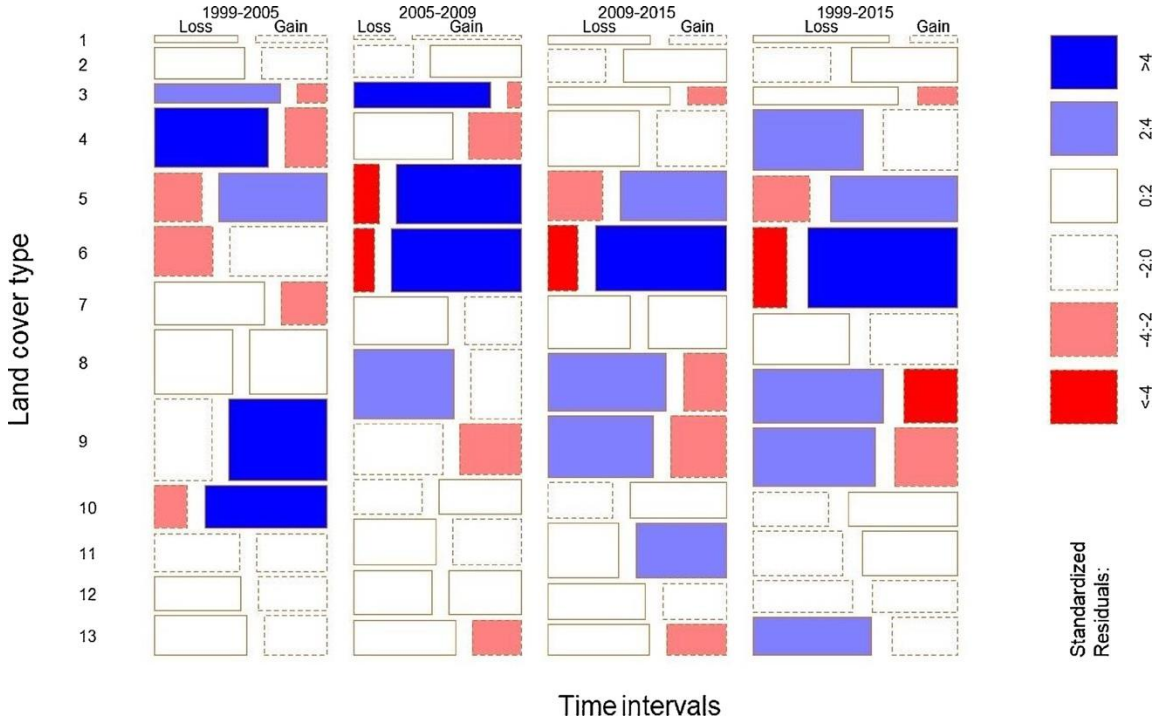

Figure 5. A mosaic plot of the land cover type loss and gain in each time interval. The land cover type numbers are, 1) open water with rivers, lakes and standing water bodies, 2) low intensity urban with paved roads, concrete, and warehouses, 3) high intensity urban with densely populated areas, 4) barren land, 5) deciduous forest, 6) evergreen forest, 7) mixed forest, 8) shrub/scrub, 9) grassland/herbaceous, 10) pasture/hay, 11) cultivated crops, 12) woody wetlands, and 13) emergent herbaceous wetlands.

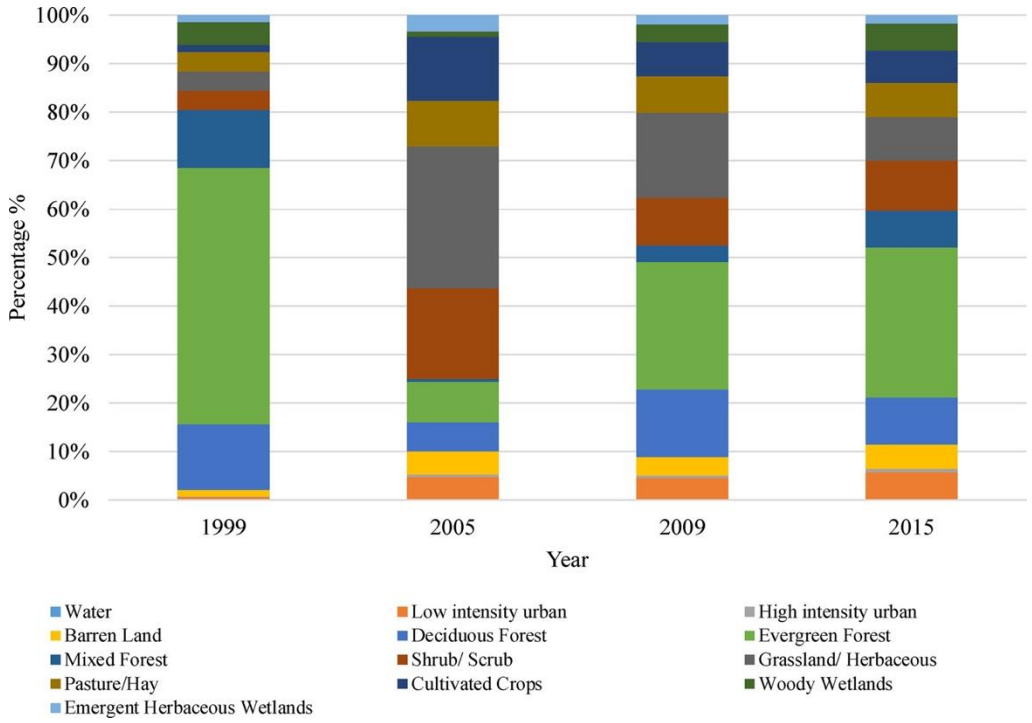

Figure 6. The comparison of a deforested area in 1999 with the land cover classification of the same area over years: 1999, 2005, 2009, and 2015.

APPENDIX B

Appendix 1. A mosaic plot comparing the per cateogry land use change at the time period between 1999-2005.

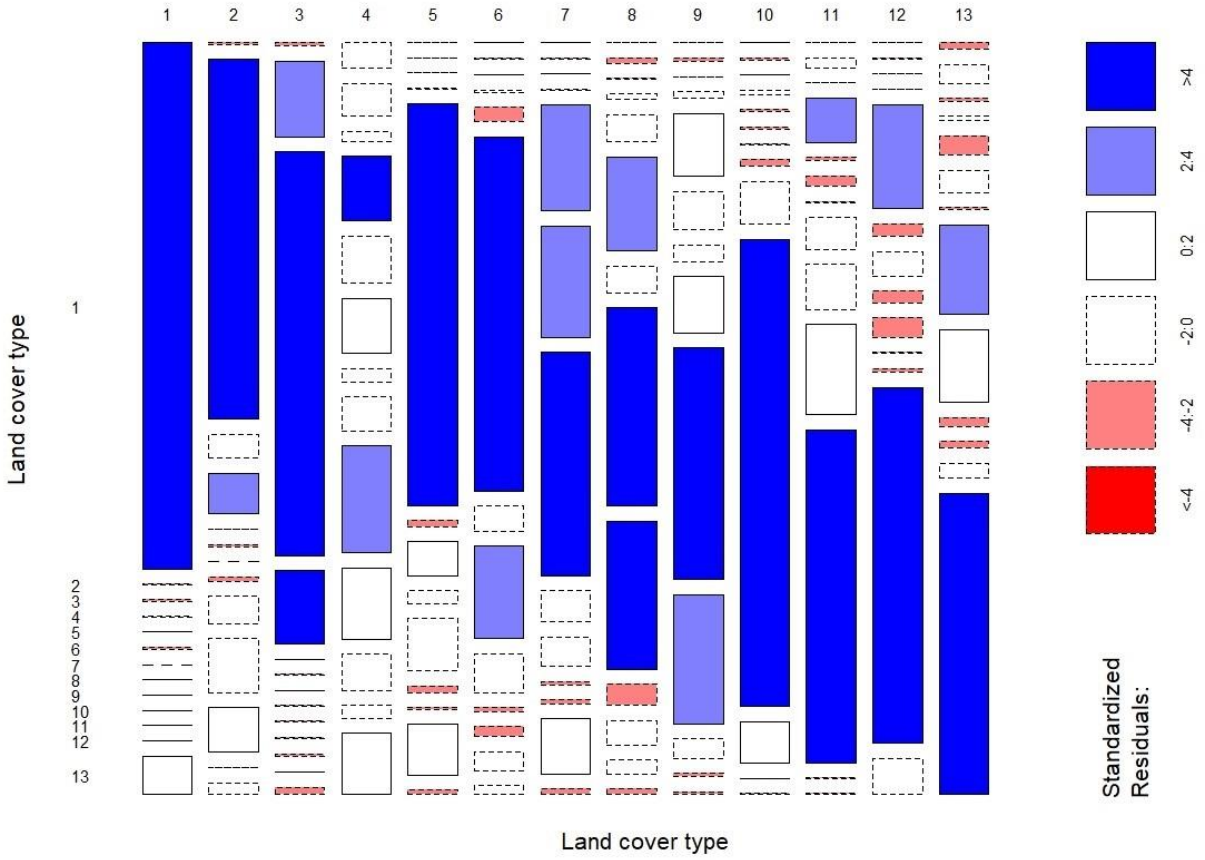

Appendix 2. A mosaic plot comparing the per cateogry land use change at the time period between 2005-2009.

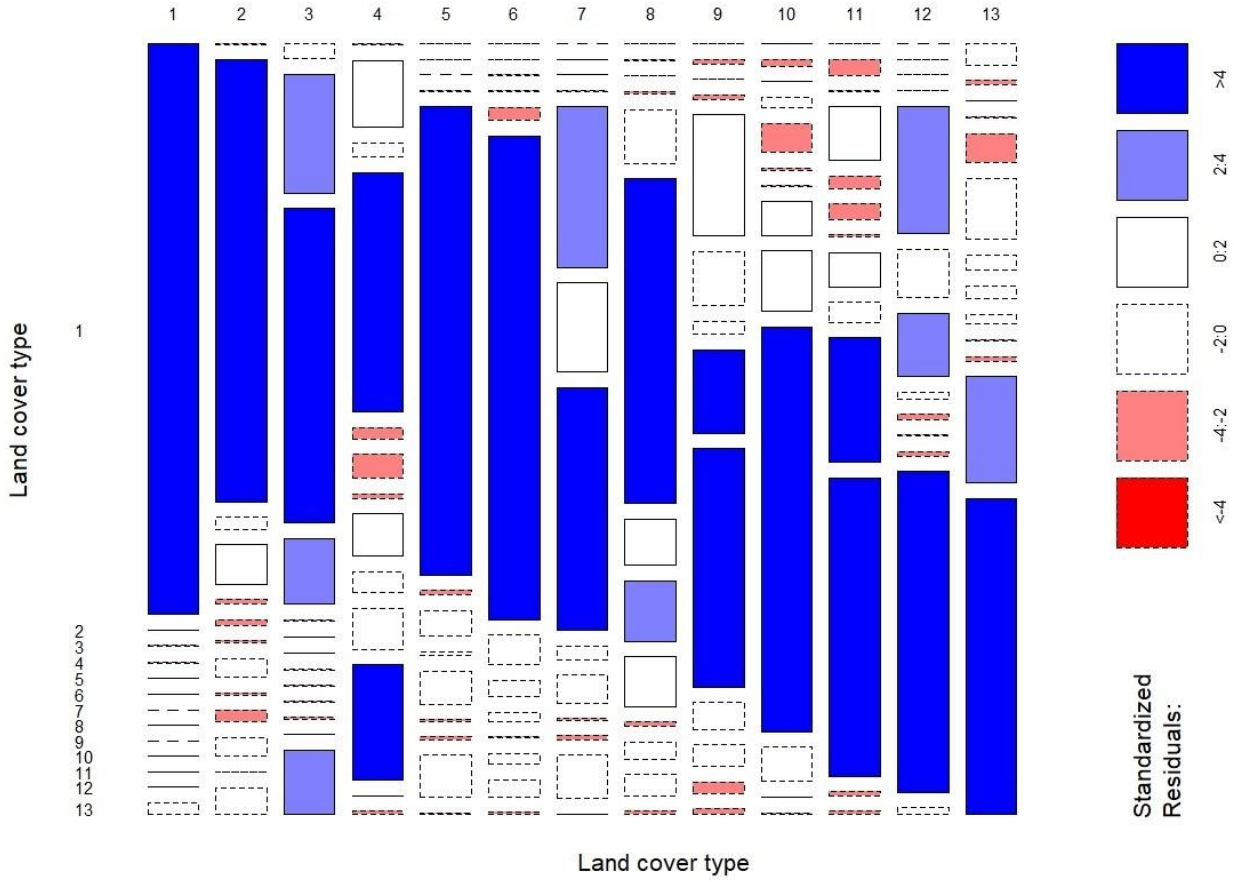

Appendix 3. A mosaic plot comparing the per cateogry land use change at the time period between 2009-2015.

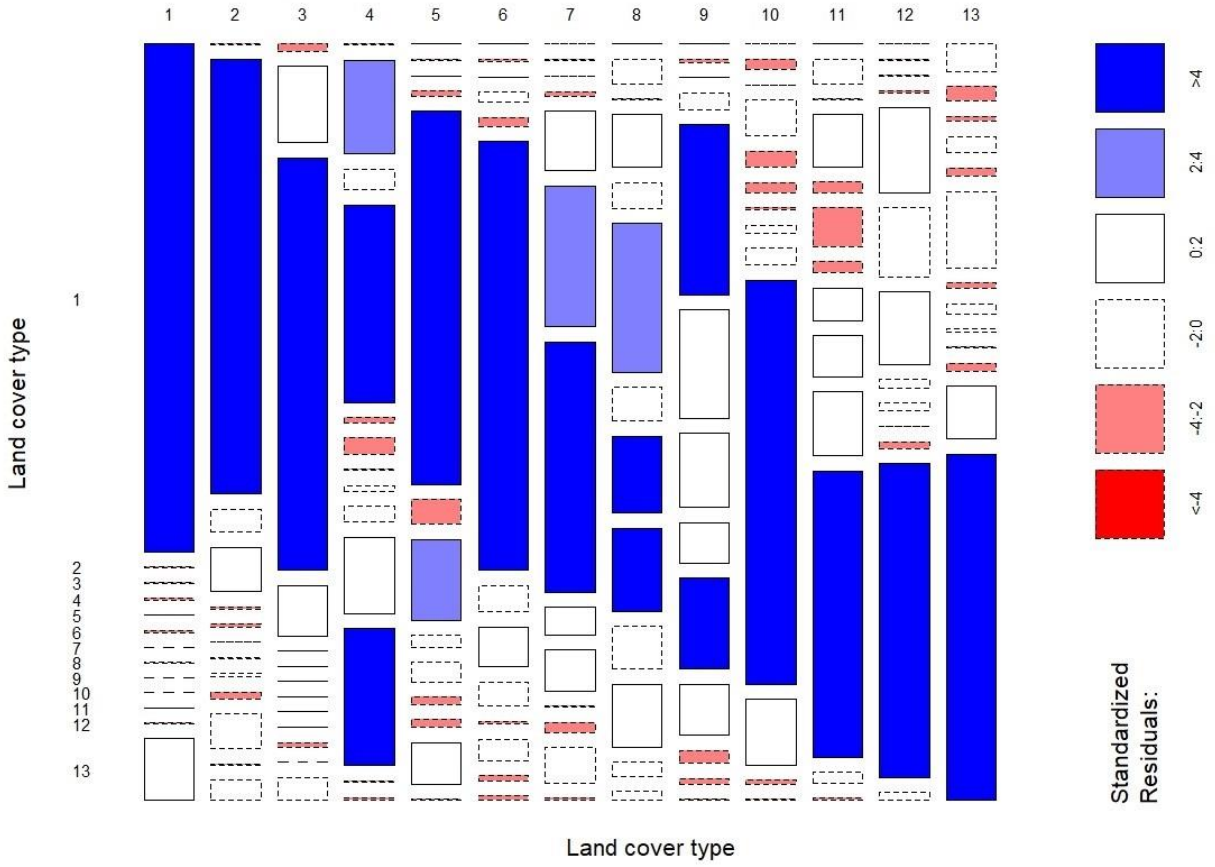

Appendix 4. A mosaic plot comparing the per cateogry land use change at the time period between 1999-2015.

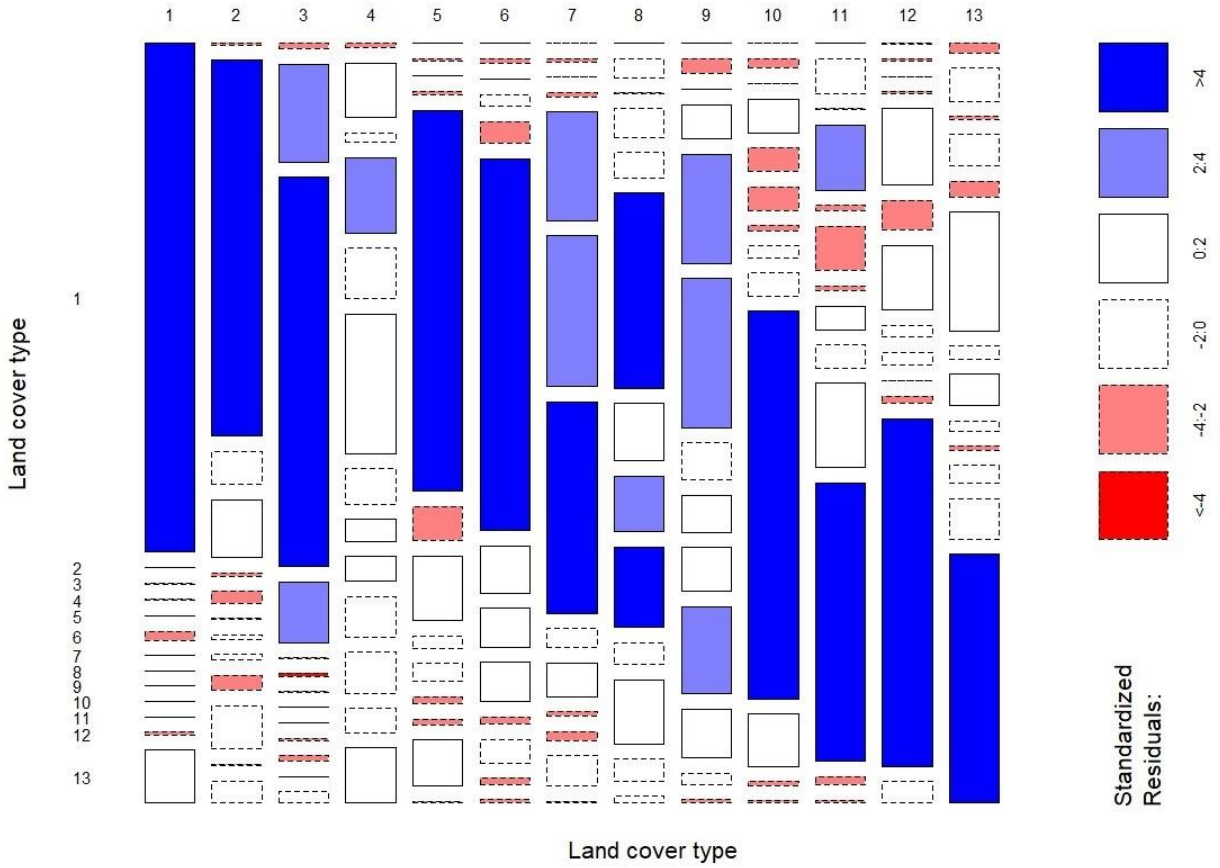

Appendix 5. Javascript code used within GEE for image classification, area calculations, and accuracy assessment.

```
//////////////////////////////////////////////////////////////////////////////////////////////////////////////////////////////////
 Land cover classification using GEE
//////////////////////////////////////////////////////////////////////
1. Study area
///// 1. Upload the study area fusion table, or draw a it in GEE
var region =
ee.FeatureCollection('ft:xxxxxxxxxxxxxxxxxxxxxxxxxxxxxxxxxxxxxx','geometry');
2. Reference data
///// 1. Import the National Agriculture Imagery Program (NAIP) image
/////      and filter the date, and the region to create the Reference data
var NAIP = ee.ImageCollection('USDA/NAIP/DOQQ')
  .filterDate('YYYY-MM-DD', 'YYYY-MM-DD')
  .filterBounds(region).mosaic();
Map.addLayer(NAIP, {}, 'NAIP DOQQ');
///// 2. Upload the reference data (training+testing) fusion table, or draw it in GEE
var reference_data = (class1).merge(class2).merge(class3).merge(class4).merge(class5)
.merge(class6).merge(class7).merge(class8).merge(class9).merge(class10).merge(class1)
.merge(class12).merge(class13);
var reference_data = reference_data.randomColumn('random', 0);
///// 3. buffer the reference data by 30 meters (each point will be buffring by 30*30 m)
```

```
var buf_ref_data = reference_data.map(function(feature) {
  return feature.buffer(30).bounds(); });
Map.addLayer(buf_ref_data,{palette:'00b300'},'buf_ref_data');
```

3. Image preprocessing

```
///// 1. Import the Digital Elevation Model (DEM) layer
var DEM = ee.Image('USGS/SRTMGL1_003').clip(region);
///// 2. Create the slope layer
var Slope = ee.Terrain.slope(DEM).rename('Slope');
///// 3. Import the Landsat images
// 3.1 filter the date, and the region
//Summer season
var start1 = '2015-06-01';//'YYYY-MM-DD'
var end1 = '2015-07-31';//'YYYY-MM-DD'
//Winter season
var start2 = '2015-12-01';//'YYYY-MM-DD'
var end2 = '2016-01-31';//'YYYY-MM-DD'
var L8_TOA = ee.ImageCollection('LANDSAT/LC8_L1T_TOA_FMASK')// or
(LANDSAT/LT5_L1T_TOA_FMASK) for other years
   .filterBounds(region)//filter the date, and the region
var L8_TOA_Summer = L8_TOA.filterDate(start1, end1);//Get only images from
Summer season
```

```
var L8_TOA_Winter = L8_TOA.filterDate(start2, end2);//Get only images from Winter
season
var L8_SR = ee.ImageCollection('LANDSAT/LC8_SR')// or (LANDSAT/LT5_SR) for
other years
   .filterBounds(region)//filter the date, and the region
var L8_SR_Summer = L8_SR.filterDate(start1, end1);//Get only images from Summer
season
var L8_SR_Winter = L8_SR.filterDate(start2, end2);//Get only images from Winter
season
// 3.2 Apply cloud mask function
//Function to remove clouds - expects the new SR data to have a cfmask layer
//The Fmask classes, with their default visualization colors are:
//0 = clear (grey), 1 = water (blue), 2 = shadow (black), 3 = snow (cyan), and 4 = cloud
(white)
var maskClouds = function(image) {
  var fmask = image.select('fmask');
  var maskImage = fmask.eq(4).or(fmask.eq(2));
  maskImage = maskImage.eq(0);
  return image.mask(maskImage);}
var L8_TOA_Summer_CloudsFree = L8_TOA_Summer.map(maskClouds)
var L8_TOA_Winter_CloudsFree = L8_TOA_Winter.map(maskClouds)
var L8_SR_Summer_CloudsFree = L8_SR_Summer.map(maskClouds)
```

```
var L8_SR_Winter_CloudsFree = L8_SR_Winter.map(maskClouds)
///// 4. Add the Tasseled Cap Transformation components (Brightness, Greenness, and
Wetness)
var calculateTasseledCap = function (image){
  var b = image.select("B1", "B2", "B3", "B4", "B5", "B7");
  var brightness_= ee.Image([0.3029, 0.2786, 0.4733, 0.5599, 0.508, 0.1872]);
  var greenness_= ee.Image([-0.2941, -0.243, -0.5424, 0.7276, 0.0713, -0.1608]);
  var wetness_= ee.Image([ 0.1511, 0.1973, 0.3283, 0.3407, -0.7117, -0.4559]);
  var sum = ee.call("Reducer.sum");
  var brightness = b.multiply(brightness_).reduce(sum);
  var greenness = b.multiply(greenness_).reduce(sum);
  var wetness = b.multiply(wetness_).reduce(sum);
  return ee.Image(brightness).addBands(greenness).addBands(wetness)};
  var L8_TC_Summer = L8_TOA_Summer_CloudsFree. mosaic();
  var L8_TC_Winter = L8_TOA_Winter_CloudsFree. mosaic();
var Summer_TasseledCap = calculateTasseledCap(L8_TC_Summer)
                    .select([0,1,2],["SBrightness","SGreenness","SWetness"])
var Winter_TasseledCap = calculateTasseledCap(L8_TC_Winter)
                    .select([0,1,2],["WBrightness","WGreenness","WWetness"])
///// 5. Generating the indices NDVI, NDBI, and MNDWI.
// 1. function to add the Normalized Difference Vegetation Index (NDVI),
// Landsat 5, and 7  ['B4','B3'] Landsat 8 ['B5','B4']
```

```
var addNDVI = function(image) {return
image.addBands(image.normalizedDifference(['B4','B3']).rename('NDVI'))};
// 2. function to add the Normalized Difference Built Index (NDBI)
// Landsat 5, and 7  ['B5','B4'] Landsat 8 ['B6','B5']
var addNDBI = function(image) {return
image.addBands(image.normalizedDifference(['B5','B4']).rename('NDBI'))};
// 3. function to add the Modified Normalized Difference Water Index (MNDWI)
// Landsat 5, and 7 ['B2','B5'] Landsat 8 ['B3','B6']
var addMNDWI = function(image) {return
image.addBands(image.normalizedDifference(['B2','B5']).rename('MNDWI'))};
// 4. Apply all the indices functions over the image collection.
var L8_SR_Summer_indices =
L8_SR_Summer_CloudsFree.map(addNDVI).map(addNDBI).map(addMNDWI).
mosaic().select(['NDVI','NDBI','MNDWI'],['SNDVI','SNDBI','SMNDWI'])
var L8_SR_Winter_indices =
L8_SR_Winter_CloudsFree.map(addNDVI).map(addNDBI).map(addMNDWI).
mosaic().select(['NDVI','NDBI','MNDWI'],['WNDVI','WNDBI','WMNDWI'])
```

4. Image classification and accuracy assessments

```
// 1. Create an image containing all bands for both seasons
// Select RBG bands ('Red','Blue','Green')
// Landsat 5, and 7  ['B5','B4'] Landsat 8 ['B4','B2','B3']
```

```
var L8_SR_Summer_RBG =
L8_SR_Summer_CloudsFree.select(['B4','B2','B3'],['SRed','SBlue','SGreen']). mosaic()
var L8_SR_Winter_RBG =
L8_SR_Winter_CloudsFree.select(['B4','B2','B3'],['WRed','WBlue','WGreen']). mosaic()
// Overlay all image bands together
var All_Bands = L8_SR_Summer_RBG
    .addBands(L8_SR_Winter_RBG)
    .addBands(Summer_TasseledCap)
    .addBands(Winter_TasseledCap)
    .addBands(L8_SR_Summer_indices)
    .addBands(L8_SR_Winter_indices)
    .addBands(DEM).addBands(Slope);
// 2. Divide the Reference data into Training (70%) and Testing (30%)
var Ref_Data = All_Bands.sampleRegions(buf_ref_data, ['class', 'random'], 30);
var training = Ref_Data.filter(ee.Filter.lte('random', 0.7));
var testing = Ref_Data.filter(ee.Filter.gt('random', 0.7));
// 3. Applying Random Forest (RF) algorithm with 500 trees and train the classifier.
var trained = ee.Classifier.randomForest(500).train(training,
'class',All_Bands.bandNames());
// Classify the image.
var classified = All_Bands.classify(trained);
// 4. Accuracy assessment
```

```
// Get a confusion matrix representing resubstitution accuracy.
var trainAccuracy = trained.confusionMatrix();
print('Resubstitution error matrix: ', trainAccuracy);
print('Training overall accuracy: ', trainAccuracy.accuracy());
// Get a confusion matrix representing expected accuracy.
var Validated = testing.classify(trained);
var testAccuracy = Validated.errorMatrix('class', 'classification');
print('Validation error matrix: ', testAccuracy);
print('Validation overall accuracy: ', testAccuracy.accuracy());
print('Validation consumer accuracy: ', testAccuracy.consumersAccuracy());
print('Validation producer accuracy: ', testAccuracy.producersAccuracy());
print('Kappa Coefficient: ', testAccuracy.kappa());
//F1 score
var CA = testAccuracy.consumersAccuracy().project([1]);
var PA = testAccuracy.producersAccuracy().project([0]);
var F1 = (CA.multiply(PA).multiply(2.0)).divide(CA.add(PA))
print("F1 score:",F1);
```

5. Calculate and print the areas

```
var areas = ee.Image.pixelArea().divide(1000 * 1000).addBands(classified)
    .reduceRegion({reducer: ee.Reducer.sum().group({
    groupField: 1, groupName:'Code',}),
    geometry: region,scale: 30,bestEffort:true,
```

```
    maxPixels: 1e9,tileScale: 16,});
print('Classification areas (km2)',  areas);
```

6. Export the classified image

```
// Export the classified image, specifying scale and region.
Export.image(classified, 'classified', {crs: 'EPSG:32133',
  scale: 30,region: region,driveFolder: "Folder_Name"});
////////////////////////////////////////////////////////////////////////////////////////////////////////////////////////////
```

CHAPTER 5

CONCLUSION

This research introduced and discussed the application of soil science education and geospatial technologies to soils and land use. Chapter two described the methodology of adaptation and evaluation of Soil Judging (Karathanasis et al., 2011) materials in Libya. It provided educational materials to practice Soil Judging using soil series description, taxonomic classes, soil forming factors, and soil chemical and physical properties in a manner that is useful for the development of education and scientific research (Che, 2013). In this chapter, a Soil Judging (Evaluation) scorecard was tested at two different universities in Libya: The University of Tripoli and the University of Zawia. Specific feedback and responses from the participants included the desire for additional seminars to increase the awareness and potential impact of Soil Judging in Libya as well as including additional field locations. Also, access to equipment including soil pH and EC tests was listed as needed.

Chapter three demonstrated a framework for classifying salt-affected soils using existing field data to interpolate and validate geospatial predictions of the classes of salt-affected soils using Geographic Information Systems (GIS). Geographic Information Systems (GIS) are a cost-effective and dependable technique for this type of research (Zurqani et al., 2018a). Understanding the different classes of the degrees of limitations to salt-affected soils is important for crop production, sustainable land use, and rehabilitation of saline soils (Yan et al., 2015; Zurqani et al., 2019a). The developed

framework classified the salt-affected soils based on electrical conductivity (ECe), soil pH, and the Sodium Adsorption Ratio (SAR) into four degrees of limitations to salt-affected soils: slight (normal soils), moderate (saline soils), severe (sodic soils), and extreme (saline-sodic soils). Most of the soils in this study were normal (slight degree of limitation). Twenty percent of the topsoil is saline-sodic (extreme degree of limitation). Future research needs should focus on predicting soil pH and sodium adsorption ratio using remote sensing techniques.

Chapter four discusses the geospatial analysis of land use change within the Savannah River basin (Zurqani et al., 2018b). The land cover maps were produced using supervised classification (random forest algorithm) for the years 1999, 2005, 2009, and 2015 in a total of the common land cover categories. This study successfully developed a regional scale analysis of land use change over the past sixteen years in the Savannah River basin by processing and comparing multiple dates of the Landsat scenes over time. The overall accuracy assessments were 79.18% (1999), 79.41% (2005), 76.04% (2009), and 76.11% (2015).

Land use change was observed as an overall trend towards the loss and gain of forested areas during all intervals of the study period. Despite the areal extent of the urban areas being much less compared to other major land cover classes, it has the potential to impact the existing land cover pattern and increment of the population in the area (Zurqani et al., 2018b; Zurqani et al., 2019b). The accelerated increase of the urbanization and the conversion of the vegetation cover, including the farmland and forests to urban development, reduce the lands that are available for food and timber

production (Wu, 2008; Zurqani et al., 2019c). Nash and Chaloud (2011) indicated that the agriculture activities, erodible soils, and urbanization negatively impacted biotic conditions in the Savannah River basin. The change detection of the land using the normalized difference vegetation index (NDVI) revealed evidence supporting the above findings. A remarkable change was observed in the forested areas by tracking the trees that were cut in 1999. The result shows an evidence of the trees' management over time in the region. This study not only discusses land use change, but also demonstrates the advantage of utilizing Google Earth Engine and the public archive database in its platform to track and monitor this change over time. In future studies, the continuous monitoring of the land use change is needed to better understand its impact in the study area, which results in more effective management strategies.

References

Che, C.A., 2013. Adaptation of regional representative soil project and soil judging for Cameroon. Clemson University.

Karathanasis, A.D., Galbraith, J.M., Shaw, J.N., Thompson, J.A., 2011. Handbook for Collegiate Soils Contest. Southeast Region Web Site: http://clic.cses.vt.edu/SE Region Soil Judging/

Nash, M.S., Chaloud, D.J., 2011. Partial least square analyses of landscape and surface water biota associations in the Savannah River Basin. Int. Scholarly Res. Netw.

Yan, N., Marschner, P., Cao, W., Zuo, C. and Qin, W., 2015. Influence of salinity and water content on soil microorganisms. International Soil and Water Conservation Research, 3(4), pp.316-323.

Wu, J., 2008. Land use changes: Economic, social, and environmental impacts. Choices 23 (4), 6–10.

Zurqani, H., Mikhailova, E., Post, C., Schlautman, M. and Sharp, J., 2018a. Predicting the Classes and Distribution of Salt-Affected Soils in Northwest Libya. Communications in Soil Science and Plant Analysis, 49(6), pp.689-700.

Zurqani, H.A., Post, C.J., Mikhailova, E.A., Schlautman, M.A. and Sharp, J.L., 2018b. Geospatial analysis of land use change in the Savannah River Basin using Google Earth Engine. International Journal of Applied Earth Observation and Geoinformation, 69, pp.175-185.

Zurqani, H.A., Mikhailova, E.A., Post, C.J., Schlautman, M.A. and Elhawej, A.R., 2019a. A Review of Libyan Soil Databases for Use within an Ecosystem Services Framework. Land, 8(5), p.82.

Zurqani, H.A., Post, C.J., Mikhailova, E.A., and Allen, J.S 2019b. Mapping Urbanization Trends in a Forested Landscape Using Google Earth Engine. Remote Sensing in Earth Systems Sciences, pp.1-10.

Zurqani, H.A., Post, C.J., Mikhailova, E.A., Cope, M.P., Allen, J.S. and Lytle, B., 2019c. Evaluating the integrity of forested riparian buffers over a large area using LiDAR data and Google Earth Engine. In Graduate Research and Discovery Symposium (GRADS). 225. Clemson University, SC, USA. https://tigerprints.clemson.edu/grads_symposium/225 (Accessed 04.10.2019).